INFLAMMATORY BOWEL DISEASES
Official Journal of the Crohn's & Colitis Foundation of America, Inc.

Reduced human α-defensin 6 in non-inflamed jejunal tissue of Crohn's disease patients

Journal:	*Inflammatory Bowel Diseases*
Manuscript ID	IBD-15-0459.R1
Wiley - Manuscript type:	Original Research Articles - Basic Science
Date Submitted by the Author:	26-Sep-2015
Complete List of Authors:	Hayashi, Ryohei; Graduate School of Biomedical & Health Sciences, Hiroshima University, Department of Gastroenterology and Metabolism Tsuchiya, Kiichiro; Graduate School Tokyo Medical and Dental University, Gastroenterology and Hepatology Fukushima, Keita; Graduate School Tokyo Medical and Dental University, Department of Gastroenterology and Hepatology Horita, Nobukatsu; Graduate School Tokyo Medical and Dental University, Department of Gastroenterology and Hepatology Hibiya, Shuji; Graduate School Tokyo Medical and Dental University, Department of Gastroenterology and Hepatology Kitagaki, Keisuke; Graduate School Tokyo Medical and Dental University, Department of Pathology Negi, Mariko; Graduate School Tokyo Medical and Dental University, Department of Pathology Itoh, Eisaku; Graduate School Tokyo Medical and Dental University, Department of Pathology Akashi, Takumi; Graduate School Tokyo Medical and Dental University, Department of Pathology Eishi, Yoshinobu; Graduate School Tokyo Medical and Dental University, Department of Pathology Okada, Eriko; Graduate School Tokyo Medical and Dental University, Department of Gastroenterology and Hepatology Araki, Akihiro; Graduate School Tokyo Medical and Dental University, Department of Gastroenterology and Hepatology Ohtsuka, Kazuo; Graduate School Tokyo Medical and Dental University, Department of Endoscopic Diagnosis and Therapy Fukuda, Shinji; RIKEN Center for Integrative Medical Sciences (IMS) AMED-CREST, Japan Agency for Medical Research and Development, Laboratory for Intestinal Ecosystem; Keio University, Institute for Advanced Biosciences Ohno, Hiroshi; RIKEN Center for Integrative Medical Sciences (IMS) AMED-CREST, Japan Agency for Medical Research and Development, Laboratory for Intestinal Ecosystem Okamoto, Ryuichi; Graduate School Tokyo Medical and Dental University, Department of Gastroenterology and Hepatology; Graduate School Tokyo Medical and Dental University, Center for Stem Cell and Regenerative Medicine; Graduate School Tokyo Medical and Dental University, Center for Stem Cell and Regenerative Medicine

	Nakamura, Testuya; Graduate School Tokyo Medical and Dental University, Department of Gastroenterology and Hepatology; Graduate School Tokyo Medical and Dental University, Department of Advanced Therapeutics for Gastrointestinal Diseases Tanaka, Shinji; Graduate School of Biomedical & Health Sciences, Hiroshima University, Endoscopy and Medicine Chayama, Kazuaki; Graduate School of Biomedical & Health Sciences, Hiroshima University, Department of Gastroenterology and Metabolism Watanabe, Mamoru; Graduate School Tokyo Medical and Dental University, Department of Gastroenterology and Hepatology
Keywords:	atonal homolog 1, mapping biopsy, Paneth cell, mucosal barrier, inflammatory bowel disease

SCHOLARONE™
Manuscripts

For Peer Review

Reduced human α-defensin 6 in non-inflamed jejunal tissue of Crohn's disease patients

Ryohei Hayashi[1, 2], Kiichiro Tsuchiya[2], Keita Fukushima[2], Nobukatsu Horita[2], Shuji Hibiya[2], Keisuke Kitagaki[3], Mariko Negi[3], Eisaku Itoh[3], Takumi Akashi[3], Yoshinobu Eishi[3], Eriko Okada[2], Akihiro Araki[2], Kazuo Ohtsuka[4], Shinji Fukuda[5, 6], Hiroshi Ohno[5], Ryuichi Okamoto[2, 7], Tetsuya Nakamura[2, 8], Shinji Tanaka[9], Kazuaki Chayama[1] and Mamoru Watanabe[2]

[1]Department of Gastroenterology and Metabolism, [9]Endoscopy and Medicine, Graduate School of Biomedical & Health Sciences, Hiroshima University, [2]Department of Gastroenterology and Hepatology, [3]Department of Pathology, [4]Department of Endoscopic Diagnosis and Therapy, [7]Center for Stem Cell and Regenerative Medicine and [8]Department of Advanced Therapeutics for Gastrointestinal Diseases, Graduate School Tokyo Medical and Dental University, [5]Laboratory for Intestinal Ecosystem, RIKEN Center for Integrative Medical Sciences (IMS) AMED-CREST, Japan Agency for Medical Research and Development, [6]Institute for Advanced Biosciences, Keio University.

Correspondence

Kiichiro Tsuchiya, M.D., Ph.D.

Associated Professor

Department of Gastroenterology and Hepatology Graduate School, Tokyo Medical and Dental University

For Peer Review

1-5-45 Yushima, Bunkyo-ku, Tokyo 113-8519, Japan

Tel: +81-3-5803-5974 Fax: +81-3-5803-0268

e-mail: kii.gast@tmd.ac.jp

Word count: 4842

Number of tables/figures: 6 figures.

Quantity of supplementary data: 5

Running title: HD6 is decreased in non-inflamed jejunum of CD patients.

Key Words: Atoh1, mapping biopsy, Paneth cell, mucosal barrier, inflammatory bowel disease

Abbreviations: Atoh1, Atonal homolog 1; IBD, inflammatory bowel disease; CD, Crohn's disease; UC, ulcerative colitis; HD6; human α-defensin 6; AMPs, secretion of antimicrobial peptides; TCF4, T-cell-specific transcription factor 4; HD, human α-defensin.

Grant support: This study was supported in part by grants-in-aid for Scientific Research, 23130506, 24590935, 25114703, 25130704 and 26221307 from the Japanese Ministry of Education, Culture, Sports, Science and Technology; Japan Foundation for Applied Enzymology; the Health and Labor Sciences Research Grants, 14526073 from the Japanese Ministry of Health, Labor and Welfare (MHLW); Research Center Network for Realization of Regenerative Medicine from Japan Science and Technology

For Peer Review

Agency (JST). Advanced Research and Development Programs for Medical Innovation from Japan Agency for Medical Research and Development (AMED)

For Peer Review

Abstract

***Background & Aims*:** Mucosal barrier dysfunction is considered a critical component of Crohn's disease (CD) pathogenesis following the identification of susceptibility genes. However, the precise mechanism underlying mucosal barrier dysfunction has not yet been elucidated. We therefore aimed to elucidate the molecular mechanism underlying the expression of human α-defensin 6 (HD6) in CD patients.

***Methods*:**

HD6 expression was induced by the transfection of an atonal homolog 1 (Atoh1) transgene and was assessed by RT-PCR. The HD6 promoter region targeted by Atoh1 and β-catenin was determined by reporter analysis and ChIP assay. HD5 / HD6 / Atoh1 / β-catenin expression in non-inflamed jejunal samples collected by balloon endoscopy from 15 CD and 9 non-IBD patients were assessed by immunofluorescence.

***Results*:**

Both promoter activity and gene expression of HD6 was significantly upregulated by the Atoh1 transgene in human colonic cancer cell line. We identified a TCF4 binding site and an E-box site critical for the regulation of HD6 transcriptional activity by directly binding of Atoh1 in the 200-bp HD6 promoter region. The treatment with beta-catenin inhibitor also decrease of HD6 promoter activity and gene expression. Moreover, HD6 expression, but not HD5 expression, was found to be decreased in non-inflamed jejunal regions from CD patients. In HD6-negative crypts, nuclear accumulation of β-catenin was impaired.

***Conclusions*:**

HD6 expression was found to be regulated by cooperation between Atoh1 and β-catenin

For Peer Review

within the HD6 promoter region. Down-regulation of HD6 in non-inflamed mucosa may contribute to mucosal barrier dysfunction of CD patients.

For Peer Review

Introduction

Ulcerative colitis (UC) and Crohn's disease (CD) are the commonest causes of inflammatory bowel disease (IBD)(1). In Western countries, there has been a recent focus on the contribution of mucosal barrier dysfunction to CD pathogenesis(2) due to the discovery of susceptibility genes, including nucleotide-binding oligomerization domain-containing protein 2 (NOD2)(3), autophagy-related protein 16-1 (ATG16L1)(4), and X-box-binding protein-1 (XBP1)(5). In particular, the function of Paneth cells in forming the mucosal barrier against gut microbiota has been considered as a critical factor in CD onset(6). Paneth cell function is broadly divided into two categories: the recognition of bacteria and the secretion of antimicrobial peptides (AMPs)(7). Although various agents are secreted by Paneth cells, the precise mechanism underlying the production of individual AMPs has yet to be clarified for the majority of AMPs. We previously reported upregulation of sPLA2 expression following activation of Notch signaling(8). The expression of human defensin 5 (HD5) is reportedly regulated by binding of β-catenin to T-cell-specific transcription factor 4 (TCF4)-binding sites(9). Human defensin 6 (HD6) is also a member of the α-defensin family and is expressed by Paneth cells(10). Because of poor antibacterial potency, the molecular mechanism underlying HD6 expression has yet not been assessed(11). However, HD6 has recently been reported to act as a mucosal barrier by forming "nanonets" to trap bacteria(12). Furthermore, reduced form of HD6 has been shown to have a bactericidal effect because HD6 expression is also important in the formation of the mucosal barrier(13). In this study, we aimed to elucidate the molecular mechanism underlying HD6

For Peer Review

expression and determine the potential role of HD6 in CD pathogenesis. We then investigated the mechanisms regulating HD6 transcriptional activity and expression contributing to decreased HD6 levels in non-inflamed jejunum of CD patients using mapping biopsies of the entire small intestine.

For Peer Review

Materials and Methods

Cell culture and chemicals

Human colon cancer-derived SW480 and DLD-1 cells were grown in Dulbecco's modified Eagle medium (Life Technologies, Grand Island, NY, USA) supplemented with 10% fetal bovine serum and 0.01% penicillin-streptomycin. Except where indicated otherwise, cells were seeded at a density of 5×10^5 cells/mL in each experiment. Cell cultures and plasmid DNA transfections were performed as previously described(14). 5μM Calphostin C (Sigma-Aldrich, St. Louis, MO, USA) was added to media to inhibit β-catenin/TCF4 complex formation(15).

Plasmids

An mCherry-Atoh1 vector was generated by inserting the *ATOH1* gene into the mCherry DNA template PG27188 (DNA 2.0, Menlo Park, CA, USA). An *ATOH1* gene mutant vector (5SA-Atoh1) was constructed by PCR-mediated mutagenesis by replacing nucleotide cording for five serine residues, TCC (160–162) and AGC (172–174, 328–330, 340–342, 352–354), with nucleotides coding for the alanine residue, GCC. The Atoh1-lentivirus vector was generated by inserting the PCR-amplified mCherry-Atoh1 or mCherry-5SA-Atoh1 plasmid into pLenti 6.4 (Invitrogen) as previously described(16). Lentiviruses were generated according to the procedure manual. A HD6 reporter plasmid was generated by cloning a 1000- and 241-bp sequence of the human HD6 gene, HD6, into a pGL4 basic vector (Promega, Madison, WI, USA). A mutant HD6 promoter was constructed using polymerase chain reaction (PCR)-mediated mutagenesis to delete TCF4-binding sites and E-box sites. The primer

For Peer Review

sequences used in this study are summarized in Supplementary Table S1.

Quantitative Real-time PCR

Total RNA was isolated using an RNeasy Micro Kit (QIAGEN), according to the manufacturer's instructions. One-microgram aliquots of total RNA were used for cDNA synthesis in 20 μl reaction volumes. One microliter of cDNA was amplified with SYBR-Green in 20 μl reactions as previously described(14). The primer sequences used in this study are summarized in Supplementary Table S1. The amount of mRNA expression was normalized by β-actin.

Luciferase Assays

SW480 cells were seeded in six-well plate culture dishes and transfected with 4 μg of reporter plasmid along with 10 ng of pRL-TK plasmid (Promega). Cells were harvested 36 h after transfection, lysed by three cycles of freezing and thawing, and the luciferase activities of each sample, measured in arbitrary units, were normalized against Renilla luciferase activities as previously described(14).

Chromatin Immunoprecipitation (ChIP) Assay

ChIP assays were performed as previously described with some modifications. DLD1 and DLD1-mCherry-Atoh1-5SA cells were seeded onto a 150-mm dish. Immunoprecipitation was performed overnight at 4°C with 10 μg of an anti-mCherry (Clontech, USA), normal mouse immunoglobulin G (sc-2025; Santa Cruz

For Peer Review

Biotechnology, Santa Cruz, CA, USA), or an anti-histone H3 antibody (Abcam, Cambridge, MA, USA). Genomic DNA fragments in immunoprecipitated samples were analyzed by PCR using primers designed against genomic DNA regions relative to the translation start site (Supplementary Table S1). Equal amounts of DNA samples were analyzed by conventional PCR in parallel using the following parameters: denaturation at 94°C for 15 s; annealing at 60°C for 30 s; and extension at 68°C for 60 s for 45 cycles. Products were resolved by agarose gel electrophoresis, stained with ethidium bromide, and visualized using an ImageQuant TL system (GE Healthcare, Milwaukee, WI, USA).

Human Small Intestinal Tissue

Human tissue specimens were obtained from 15 CD and 9 non-IBD patients with an indication to undergo double balloon endoscopy or single balloon endoscopy at Tokyo Medical and Dental University Hospital. Patient's information is shown in Supplementary Table S2. Non-IBD patients were performed endoscopy because of the obscure gastrointestinal bleeding. To analyze the structure of normal small intestine, we selected biopsy specimens from non-IBD patients who showed no abnormality in small intestine(17). Written informed consent was obtained from all included patients and this study was approved by the Ethics Committee of Tokyo Medical and Dental University.

Microarray analysis

For Peer Review

Total RNA was extracted using standard protocols (Affymetrix). Targets were prepared and hybridized to GeneChip Human Gene 1.0 ST arrays (Affymetrix), according to standard protocols. GeneChip data sets were analyzed using GeneSpring GX 7.3.1 (Agilent). Array data were normalized using robust multi-array analysis considering guanine and cytosine content algorithms (18). This result was assigned the GEO accession number GSE69762.

Immunohistochemistry

Immunohistochemical analysis of human small intestine was conducted using paraffin-embedded and frozen sections. Tissue sections were stained following microwave treatment (500W, 10 min) in 10 mM citrate buffer. An Atoh1 antibody, originally generated by immunizing rabbits with Atoh1 peptide, were used as previously described(17). Anti-HD6 (Atlas Antibodies) and anti-β-catenin (BD Biosciences) antibodies were also used. Primary antibodies were visualized using secondary antibodies conjugated to either Alexa-594 or Alexa-488 (Life Technologies). Sections were mounted using VectaShield mounting medium containing DAPI (Vector Laboratories) and visualized by confocal laser fluorescent microscopy (FLUOVIEW FV10i;Olympus) as previously described(19).

Statistical Analyses

Quantitative real-time PCR analyses were statistically analyzed using the Student's t-

For Peer Review

test. P-values <0.05 were considered statistically significant. In the cases of more than two data sets existed, differences between groups were determined using one-way analysis of variance (ANOVA) and Bonferroni's post hoc method of multiple comparisons.

For Peer Review

Results

Atoh1 upregulates HD6 expression and transcriptional activity

To assess the expression of Paneth cell phenotypic genes in response to Atoh1, we transiently transfected the *ATOH1* gene into SW480 cells, resulting in marked upregulation of HD6 only in response to Atoh1 (Fig. 1a). We therefore investigated the HD6 promoter region. As there are three TCF4-binding sites and four E-box-binding sites within 1000 bp of the HD6 promoter region (Fig. 1b), we constructed two reporter plasmids to assess HD6 transcriptional activity (Fig. 1c). Reporter analysis demonstrated significant upregulation of HD6 transcriptional activity by Atoh1 within 241 bp of the HD6 promoter region in addition to 1000 bp of the HD6 promoter region (Fig. 1d).

An E-box-binding site within the HD6 promoter is crucial for the transcriptional regulation by Atoh1

We then investigated the three TCF-binding sites within 1000 bp of the HD6 promoter region has previously been reported to be regulated by β-catenin via TCF-binding sites. Deletion mutation of the TCF-binding sites demonstrated the TCF-binding site at 178 bp (T3) was significantly affected transcriptional regulation of HD6 by Atoh1 (Fig. 2a). As Atoh1 recognizes and binds to the E-box sequence(20), we constructed E-box deletion mutants of HD6 reporter plasmids. Deletion mutation of the E-box-binding site demonstrated the E-box-binding site at 101 bp (E3) significantly affected transcriptional regulation of HD6 by Atoh1 (Fig. 2b). Deletion of both T3 and E3 resulted in significantly decreased HD6 transcriptional activity compared to individual deletions (Fig. 2c), indicating that E3 and T3 may be crucial for Atoh1-induced HD6 expression.

For Peer Review

Atoh1 directly binds to the HD6 promoter region

We next assessed whether Atoh1 directly binds to the HD6 promoter region. We generated stable DLD1 cell lines that strongly expressed Atoh1 protein as previously described (mCherry 5SA Atoh1)(16). We then designed primers for ChIP assays as shown in Fig. 3a. ChIP assays demonstrated the direct binding of Atoh1 within 200 bp of the HD6 promoter region (Fig. 3b).

β-catenin regulates HD6 expression in cooperation with Atoh1

As DLD1 and SW480 cells are generated from human colon cancer with APC gene deletions, nuclear accumulation of β-catenin protein is observed in these cells. The presence of β-catenin alone was not found to induce HD6 expression (Fig. 1a). We therefore assessed the effect of β-catenin on Atoh1-induced HD6 expression. Treatment with calphostin C, an inhibitor of the binding of β-catenin to TCF4, resulted in decreased levels of cyclin D1. Treatment of Atoh1-expressing cells with calphostin C led to decreased HD6 expression with no effect on TCF4 expression (Fig. 4a). Calphostin C also caused decreased Atoh1-induced HD6 transcriptional activity (Fig. 4b). Interestingly, calphostin C was shown to decrease transcriptional activity in response to the TCF4-binding site deletion mutant, indicating β-catenin may regulate HD6 expression via the E-box biding site (E3) in cooperation with Atoh1 (Fig. 4c).

Atoh1 protein colocalizes with β-catenin in HD6-expressing Paneth cells

We next assessed the localization of Atoh1 and β-catenin in human Paneth cells. β-catenin was found to be expressed in the nuclei of crypt base cells, whereas Atoh1 was

For Peer Review

expressed in the nuclei of almost all epithelial cells (Fig. 5a). Double immunostaining for HD6 and Atoh1 also demonstrated nuclear expression of Atoh1 in HD6-expressing cells (Fig. 5b). Double immunostaining for HD6 and β-catenin demonstrated nuclear accumulation of β-catenin in HD6-expressing cells demonstrating colocalization of Atoh1 and β-catenin in HD6 expressing Paneth cells (Fig. 5c). Moreover, double immunostaining for HD5 and β-catenin demonstrated nuclear accumulation of β-catenin in HD5-expressing cells demonstrating colocalization of Atoh1 and β-catenin in HD5 expressing Paneth cells (Fig. 5d). Furthermore, double immunostaining for HD5 and HD6 demonstrated that HD6 and HD5 were expressed in the same cells in almost Paneth cells (Supplementary Figure S1a). However, HD6 single positive cell was detected in some crypts (Supplementary Figure S1b).

The HD6 expression is decreased in non-inflamed jejunum of CD patients due to impaired nuclear accumulation of β-catenin

Finally, we assessed HD6 expression in biopsy specimens from CD patients. To exclude the effect of inflammation, we performed microarray analysis using biopsy specimens (Supplementary Table S3). No significant upregulation of inflammation-related genes were detected in jejunal tissue from CD patients compared to non-IBD patients, whereas numerous inflammation-related genes were increased in biopsies taken from throughout the ileum of CD patients, suggesting that the jejunal state might reflect CD pathogenesis of intestinal epithelial cells without mucosal damage by the inflammation. No significant difference in the number of Paneth cells per crypt was observed between jejunal biopsies from CD and non-IBD patients (Figs. 6a,b). Interestingly, immunostaining for HD6 demonstrated markedly decreased levels of HD6

For Peer Review

in jejunal samples from CD patients (Fig. 6c). The number of HD6-positive cells per crypt was decreased in jejunal biopsies from CD patients. There was no difference in the number of HD5-positive cells per crypt between jejunal samples from CD and non-IBD patients (Figs. 6d,e). HD6-expressing cells were found to be entirely absent in a proportion of crypts in jejunal samples from CD patients (Fig 6d). We therefore further assessed the mechanisms underlying the presence of 8 HD6-negative crypts in 6 CD patients. Immunostaining demonstrated nuclear accumulation of β-catenin was impaired in all HD6-negative crypts, whereas nuclear expression of Atoh1 was observed in all cells (Fig. 6f) (Supplementary Figure S2).

Discussion

This study demonstrated regulation of HD6 expression by the binding of Atoh1 to an E-box-binding site in cooperation with β-catenin binding to a TCF4-binding site and an E-box-binding site in the HD6 promoter region. We further demonstrated decreased levels of HD6 in non-inflamed jejunal biopsy samples from CD patients due to impaired nuclear localization of β-catenin, but not Atoh1.

Previous studies have suggested β-catenin might regulate the HD6 expression in a similar manner to HD5 as β-catenin has also been shown to bind to the HD6 promoter region(21). However, β-catenin has yet to be shown to promote HD6 expression. Although ATOH1 expression is crucial for differentiation toward secretary cell lineages, including Paneth cells(22), whether ATOH1 also regulates expression of Paneth phenotypic genes remains unknown. In the present study, we demonstrate for the first time that HD6 expression is directly regulated by Atoh1 in cooperation with β-catenin. We further identified critical sequences allowing binding of Atoh1 and β-catenin to the

For Peer Review

HD6 promoter region resulting in HD6 gene transcription. Treatment with calphostin C, a β-catenin inhibitor, completely inhibited the expression and transcriptional activity of HD6. Deletion of the TCF4-binding site partially blocked the transcriptional activity of HD6, indicating β-catenin might regulate HD6 transcriptional activity via E-box-binding site in cooperation with Atoh1, in addition to binding to the TCF4-binding site. The interaction between Atoh1 and β-catenin remains unclear with more detailed future studies required to fully elucidate their contribution to the regulation of HD6 expression in Paneth cells. Moreover, individual Paneth phenotypic genes encoding products, such as HD5, lysozyme, and sPLA2 may be independently regulated suggesting that Paneth cell subtypes may exist that maintain homeostasis throughout the entire small intestine.

Interestingly, expression of HD6, but not HD5, was decreased in non-inflamed jejunal biopsies from CD patients. We performed gene expression pattern analysis of the entire small intestine of non-IBD patients using biopsy specimens collected by balloon-assisted enteroscopy(17). In this study, we collected biopsy specimens from the entire small intestine of CD patients in order to compare gene expression to tissues obtained from non-IBD patients. Numerous inflammation-related genes were found to be significantly increased in the whole ileum of CD patients compared with samples taken from corresponding regions in non-IBD patients. In particular, inflammation-related genes were upregulated in the proximal ileum regardless of endoscopic and pathological findings. Jejunal non-inflamed mucosa was selected based on endoscopic, pathological, and molecular findings to assess the primary pathogenesis of CD. Microarray analysis of jejunal tissue from four CD patients demonstrated no upregulation of inflammation-related genes compared to non-IBD patients. Consequently, we able to demonstrate decreased numbers of HD6-positive cells, but not HD5-positive cells, without an

For Peer Review

inflammatory effect in CD patients. We found the nuclear accumulation of β-catenin was impaired in HD6-negative crypts suggesting HD6 expression was suppressed due to decreased β-catenin, but not Atoh1, activity while the number of Paneth cells remained constant. It has been reported that HD6 is secreted as an oxidized peptide from the bottom of crypts into an aerobic environment and can be spontaneously reduced upon reaching the reducing environment of the intestinal lumen(13). Therefore, mucosal barrier dysfunction may occur in CD patients despite normal pathological findings. This process may be particularly relevant in Japanese CD patients with genetic variants affecting mucosal barrier function, such as NOD2(23) and ATG16L1(24), as a fundamental mechanism underlying the pathogenesis of CD. It should be considered that CD treatments may affect non-inflamed mucosa. However, assessment of the mucosa prior to the onset of CD using a prospective study is not possible, as we believe non-inflamed jejunal mucosa mimics findings prior to CD onset. Large-scale studies that include Caucasian and Asian patients are required to confirm this hypothesis.

In this study, Atoh1 expression was not altered in jejunum mucosa without the effect of inflammation. It has however been reported that HD6 expression was reduced in inflamed ileum(25) with aberrant Notch signal activation(26). Because Atoh1 is directly suppressed by Hes1 via Notch signaling(14), Atoh1 might be decreased in inflamed ileum of CD patients, resulting in the reduced HD6 expression in corporation with the impairment of β-catenin. In future, more detailed analysis for Atoh1 expression in inflamed ileum is also required to understand the mucosal barrier dysregulation in entire small intestine of CD patients.

In conclusion, HD6 is required for the nuclear accumulation of both Atoh1 and β-catenin in Paneth cells. Decreased levels of nuclear β-catenin, but not Atoh1, induce

For Peer Review

decreased levels of HD6 without impairment of epithelial differentiation toward Paneth cells in CD. Further studies of non-inflamed mucosa may further elucidate the mechanisms underlying the pathogenesis of CD.

Disclosures: The authors disclose no conflict of interest.

For Peer Review

References

1. Kaser A, Zeissig S, Blumberg R. Inflammatory bowel disease. Annu Rev Immunol. 2010;28:573-621

2. Maloy KJ, Powrie F. Intestinal homeostasis and its breakdown in inflammatory bowel disease. Nature. 2011;474:298-306

3. Strober W, Watanabe T. NOD2, an intracellular innate immune sensor involved in host defense and Crohn's disease. Mucosal Immunol. 2011;4:484-495

4. Cadwell K, Liu JY, Brown SL, et al. A key role for autophagy and the autophagy gene Atg16l1 in mouse and human intestinal Paneth cells. Nature. 2008;456:259-263

5. Kaser A, Lee AH, Franke A, et al. XBP1 links ER stress to intestinal inflammation and confers genetic risk for human inflammatory bowel disease. Cell. 2008;134:743-756

6. Jager S, Stange EF, Wehkamp J. Inflammatory bowel disease: an impaired barrier disease. Langenbecks Arch Surg. 2013;398:1-12

7. Clevers HC, Bevins CL. Paneth cells: maestros of the small intestinal crypts. Annu Rev Physiol. 2013;75:289-311

8. Okamoto R, Tsuchiya K, Nemoto Y, et al. Requirement of Notch activation during regeneration of the intestinal epithelia. Am J Physiol Gastrointest Liver Physiol. 2009;296:G23-35

9. van Es JH, Jay P, Gregorieff A, et al. Wnt signalling induces maturation of Paneth cells in intestinal crypts. Nat Cell Biol. 2005;7:381-386

10. Jones DE, Bevins CL. Defensin-6 mRNA in human Paneth cells: implications for antimicrobial peptides in host defense of the human bowel. FEBS Lett.

For Peer Review

1993;315:187-192

11. Ericksen B, Wu Z, Lu W, et al. Antibacterial activity and specificity of the six human {alpha}-defensins. Antimicrob Agents Chemother. 2005;49:269-275

12. Chu H, Pazgier M, Jung G, et al. Human α-defensin 6 promotes mucosal innate immunity through self-assembled peptide nanonets. Science. 2012;337:477-481

13. Schroeder BO, Ehmann D, Precht JC, et al. Paneth cell alpha-defensin 6 (HD-6) is an antimicrobial peptide. Mucosal Immunol. 2015;8:661-671

14. Zheng X, Tsuchiya K, Okamoto R, et al. Suppression of hath1 gene expression directly regulated by hes1 via notch signaling is associated with goblet cell depletion in ulcerative colitis. Inflamm Bowel Dis. 2011

15. Lepourcelet M, Chen YN, France DS, et al. Small-molecule antagonists of the oncogenic Tcf/beta-catenin protein complex. Cancer Cell. 2004;5:91-102

16. Kano Y, Tsuchiya K, Zheng X, et al. The acquisition of malignant potential in colon cancer is regulated by the stabilization of Atonal homolog 1 protein. Biochem Biophys Res Commun. 2013;432:175-181

17. Iwasaki M, Tsuchiya K, Okamoto R, et al. Longitudinal cell formation in the entire human small intestine is correlated with the localization of Hath1 and Klf4. J Gastroenterol. 2011;46:191-202

18. Fukuda S, Toh H, Hase K, et al. Bifidobacteria can protect from enteropathogenic infection through production of acetate. Nature. 2011;469:543-547

19. Horita N, Tsuchiya K, Hayashi R, et al. Fluorescent labelling of intestinal epithelial cells reveals independent long-lived intestinal stem cells in a crypt. Biochem Biophys Res Commun. 2014;454:493-499

20. Akazawa C, Ishibashi M, Shimizu C, et al. A mammalian helix-loop-helix

For Peer Review

factor structurally related to the product of Drosophila proneural gene atonal is a positive transcriptional regulator expressed in the developing nervous system. J Biol Chem. 1995;270:8730-8738

21. Wehkamp J, Wang G, Kubler I, et al. The Paneth cell alpha-defensin deficiency of ileal Crohn's disease is linked to Wnt/Tcf-4. J Immunol. 2007;179:3109-3118

22. Yang Q, Bermingham N, Finegold M, et al. Requirement of Math1 for secretory cell lineage commitment in the mouse intestine. Science. 2001;294:2155-2158

23. Inoue N, Tamura K, Kinouchi Y, et al. Lack of common NOD2 variants in Japanese patients with Crohn's disease. Gastroenterology. 2002;123:86-91

24. Yamazaki K, Onouchi Y, Takazoe M, et al. Association analysis of genetic variants in IL23R, ATG16L1 and 5p13.1 loci with Crohn's disease in Japanese patients. J Hum Genet. 2007;52:575-583

25. Wehkamp J, Salzman NH, Porter E, et al. Reduced Paneth cell alpha-defensins in ileal Crohn's disease. Proc Natl Acad Sci U S A. 2005;102:18129-18134

26. Dahan S, Rabinowitz KM, Martin AP, et al. Notch-1 signaling regulates intestinal epithelial barrier function, through interaction with CD4+ T cells, in mice and humans. Gastroenterology. 2011;140:550-559

For Peer Review

Figure Legends

Figure 1. Atoh1 up regulates *HD6* expression and transcriptional activity

(a) mCherry-Atoh1 or GFP was transfected into SW480 cells. After 48 h, the expression of human AMPs was determined by RT-PCR. The amount of mRNA expression was normalized by β-actin. Statistical analysis was used Student's t-test. *p < 0.05, **p < 0.01, ***p < 0.001, n = 3. N.S.: not significant. (b) Schematic representation of the HD6 promoter region. There are three TCF4-binding sites (T/A-T/A-CAAAG) and four E-box-binding sites (CANNTG) within 1000 bp. (c) Schematic representation of HD6 reporter plasmids. We constructed two different lengths of the HD6 promoter region, 1000 bp and 241 bp, respectively. Each binding sites were numbered. (d) HD6 reporter activity of by Atoh1 was analyzed. Atoh1 significantly promoted the reporter activity of a 241-bp HD6 promoter region as well as a 1000-bp HD6 promoter region. Statistical analysis was used one-way analysis of variance (ANOVA) and Bonferroni's post hoc method. *p < 0.05, **p < 0.01, ***p < 0.001, n = 3. N.S.: not significant.

Figure 2. An E-box-binding site on HD6 promoter is crucial for the transcriptional activity by Atoh1

(a) All or each TCF4-binding sites within 1000 bp of the HD6 promoter region were deleted by mutagenesis. Each reporter plasmids were transfected with Atoh1 into SW480 cells. 48 h after transfection, reporter assay showed significant suppression of transcriptional activity in the T3 deletion mutant as well as that in the deletion mutant of all TCF4-binding sites. (b) All or each E-box-binding sites within 241 bp of the HD6

For Peer Review

promoter region were deleted by mutagenesis. Each reporter plasmids was transfected with Atoh1 into SW480 cells. Forty-eight hours after transfection, reporter assay showed significant suppression of transcriptional activity in the E3 deletion mutant, which was almost identical to that in the deletion mutant of all E-box-binding sites. Statistical analysis was used one-way analysis of variance (ANOVA) and Bonferroni's post hoc method. *p < 0.05, **p < 0.01, ***p < 0.001, n = 3. N.S.: not significant.

Figure 3. Atoh1 directly binds the HD6 promoter region

(a) ChIP assay was performed using DLD1 cells with or without mCherry 5SA-Atoh1. Each region is indicated by a schematic. (b) Each region was amplified from the immunoprecipitant by each antibody. Only the region including the 13–290-bp segment of the HD6 promoter (region b) was amplified from the immunoprecipitant by the mCherry antibody. H3: anti-histone 3 antibody was used as positive control.

Figure 4. β-catenin also regulates the HD6 expression in cooperation with Atoh1

(a) β-catenin inhibitors were transfected into mCherry 5SA-Atoh1 DLD1 cells for 48 h. The expression of each gene was analyzed by RT-PCR. The amount of mRNA expression was normalized by β-actin. Statistical analysis was used Student's t-test. *p < 0.05, **p < 0.01, ***p < 0.001, n = 3. N.S.: not significant. (b, c) Each reporter plasmid was transfected into mCherry 5SA-Atoh1 DLD1 cells with either DMSO or β-catenin inhibitor. Forty-eight hours after transfection, the reporter activity was assessed. Statistical analysis was used one-way analysis of variance (ANOVA) and Bonferroni's post hoc method. *p < 0.05, **p < 0.01, ***p < 0.001, n = 3. N.S.: not significant.

For Peer Review

Figure 5. Atoh1 protein is colocalized with β-catenin in HD6-expressing Paneth cells

(a) Immunofluorescence double-staining of Atoh1 and β-catenin in human intestine of non-IBD patients merged with DAPI showed colocalization of Atoh1 and β-catenin in nuclei (arrow head). Scale bar, 10 μm. (b) Immunofluorescence double-staining of HD6 and Atoh1 in human intestine of non-IBD patients merged with DAPI showed nuclear expression of Atoh1 in HD6-expressing cells. Scale bar, 10 μm. (c) Immunofluorescence double-staining of HD6 and β-catenin in human intestine of non-IBD patients merged with DAPI showed nuclear accumulation of β-catenin in HD6-expressing cells (arrow head). Scale bar, 10 μm. (d) Immunofluorescence double-staining of HD5 and β-catenin in human intestine of non-IBD patients merged with DAPI showed nuclear accumulation of β-catenin in HD5-expressing cells (arrow head). Scale bar, 10 μm.

Figure 6. HD6 expression decreased in non-inflamed jejunum of CD patients due to impairing the nuclear accumulation of β-catenin

(a) HE-staining of jejunal specimen taken from CD patients or healthy control. Paneth cells are located at the base of crypt shown as a cell with large eosinophilic refractile granules in cytoplasm. Scale bar, 10 μm. (b) The average number of Paneth cells per a crypt in the CD or non-IBD patients. The number of Paneth cells was counted at over 10 crypts/person. (c) Immunofluorescence analysis of HD6 merged with DAPI in non-inflamed jejunum of CD or non-IBD patients. Scale bar, left panel; 500 μm, right panel; 10 μm. (d) The number of HD5- or HD6-positive cells per crypt in the CD or non-IBD

For Peer Review

patients. The positive crypt of HD5 was investigated in 213 crypts of 9 non-IBD patients and 377 crypts of 15 CD patients, respectively. The positive crypt of HD6 was investigated in 248 crypts of 9 non-IBD patients and 391 crypts of 15 CD patients, respectively. (e) The average number of HD5- or HD6- positive cells per crypt in the CD or non-IBD patients. The number of Paneth cells was counted at over 10 crypts/person. (f) Immunofluorescence analysis of HD6 either with β-catenin or Atoh1 merged with DAPI in non-inflamed jejunum of CD patients. Nuclear accumulation of β-catenin was impaired in all HD6 negative crypts. Scale bar, 10 μm. Atoh1 expression was not changed despite HD6 expression. Arrow heads point to HD6 positive cells. Statistical analysis was used Student's t-test. **$p < 0.01$, ***$p < 0.001$. N.S.: not significant.

For Peer Review

Reduced human α-defensin 6 in non-inflamed jejunal tissue of Crohn's disease patients

Ryohei Hayashi[1, 2], Kiichiro Tsuchiya[2], Keita Fukushima[2], Nobukatsu Horita[2], Shuji Hibiya[2], Keisuke Kitagaki[3], Mariko Negi[3], Eisaku Itoh[3], Takumi Akashi[3], Yoshinobu Eishi[3], Eriko Okada[2], Akihiro Araki[2], Kazuo Ohtsuka[4], Shinji Fukuda[5, 6], Hiroshi Ohno[5], Ryuichi Okamoto[2, 7], Tetsuya Nakamura[2, 8], Shinji Tanaka[9], Kazuaki Chayama[1] and Mamoru Watanabe[2]

[1]Department of Gastroenterology and Metabolism, [9]Endoscopy and Medicine, Graduate School of Biomedical & Health Sciences, Hiroshima University, [2]Department of Gastroenterology and Hepatology, [3]Department of Pathology, [4]Department of Endoscopic Diagnosis and Therapy, [7]Center for Stem Cell and Regenerative Medicine and [8]Department of Advanced Therapeutics for Gastrointestinal Diseases, Graduate School Tokyo Medical and Dental University, [5]Laboratory for Intestinal Ecosystem, RIKEN Center for Integrative Medical Sciences (IMS) AMED-CREST, Japan Agency for Medical Research and Development, [6]Institute for Advanced Biosciences, Keio University.

Correspondence

Kiichiro Tsuchiya, M.D., Ph.D.

Associated Professor

Department of Gastroenterology and Hepatology Graduate School, Tokyo Medical and Dental University

For Peer Review

1-5-45 Yushima, Bunkyo-ku, Tokyo 113-8519, Japan

Tel: +81-3-5803-5974 Fax: +81-3-5803-0268

e-mail: kii.gast@tmd.ac.jp

Word count: 4842

Number of tables/figures: 6 figures.

Quantity of supplementary data: 5

Running title: HD6 is decreased in non-inflamed jejunum of CD patients.

Key Words: Atoh1, mapping biopsy, Paneth cell, mucosal barrier, inflammatory bowel disease

Abbreviations: Atoh1, Atonal homolog 1; IBD, inflammatory bowel disease; CD, Crohn's disease; UC, ulcerative colitis; HD6; human α-defensin 6; AMPs, secretion of antimicrobial peptides; TCF4, T-cell-specific transcription factor 4; HD, human α-defensin.

Grant support: This study was supported in part by grants-in-aid for Scientific Research, 23130506, 24590935, 25114703, 25130704 and 26221307 from the Japanese Ministry of Education, Culture, Sports, Science and Technology; Japan Foundation for Applied Enzymology; the Health and Labor Sciences Research Grants, 14526073 from the Japanese Ministry of Health, Labor and Welfare (MHLW); Research Center Network for Realization of Regenerative Medicine from Japan Science and Technology

For Peer Review

Agency (JST). Advanced Research and Development Programs for Medical Innovation from Japan Agency for Medical Research and Development (AMED)

For Peer Review

Abstract

***Background & Aims*:** Mucosal barrier dysfunction is considered a critical component of Crohn's disease (CD) pathogenesis following the identification of susceptibility genes. However, the precise mechanism underlying mucosal barrier dysfunction has not yet been elucidated. We therefore aimed to elucidate the molecular mechanism underlying the expression of human α-defensin 6 (HD6) in CD patients.

***Methods*:**

HD6 expression was induced by the transfection of an atonal homolog 1 (Atoh1) transgene and was assessed by RT-PCR. The HD6 promoter region targeted by Atoh1 and β-catenin was determined by reporter analysis and ChIP assay. HD5 / HD6 / Atoh1 / β-catenin expression in non-inflamed jejunal samples collected by balloon endoscopy from 15 CD and 9 non-IBD patients were assessed by immunofluorescence.

***Results*:**

Both promoter activity and gene expression of HD6 was significantly upregulated by the Atoh1 transgene in human colonic cancer cell line. We identified a TCF4 binding site and an E-box site critical for the regulation of HD6 transcriptional activity by directly binding of Atoh1 in the 200-bp HD6 promoter region. The treatment with beta-catenin inhibitor also decrease of HD6 promoter activity and gene expression. Moreover, HD6 expression, but not HD5 expression, was found to be decreased in non-inflamed jejunal regions from CD patients. In HD6-negative crypts, nuclear accumulation of β-catenin was impaired.

***Conclusions*:**

HD6 expression was found to be regulated by cooperation between Atoh1 and β-catenin

For Peer Review

within the HD6 promoter region. Down-regulation of HD6 in non-inflamed mucosa may contribute to mucosal barrier dysfunction of CD patients.

For Peer Review

Introduction

Ulcerative colitis (UC) and Crohn's disease (CD) are the commonest causes of inflammatory bowel disease (IBD)(1). In Western countries, there has been a recent focus on the contribution of mucosal barrier dysfunction to CD pathogenesis(2) due to the discovery of susceptibility genes, including nucleotide-binding oligomerization domain-containing protein 2 (NOD2)(3), autophagy-related protein 16-1 (ATG16L1)(4), and X-box-binding protein-1 (XBP1)(5). In particular, the function of Paneth cells in forming the mucosal barrier against gut microbiota has been considered as a critical factor in CD onset(6). Paneth cell function is broadly divided into two categories: the recognition of bacteria and the secretion of antimicrobial peptides (AMPs)(7). Although various agents are secreted by Paneth cells, the precise mechanism underlying the production of individual AMPs has yet to be clarified for the majority of AMPs. We previously reported upregulation of sPLA2 expression following activation of Notch signaling(8). The expression of human defensin 5 (HD5) is reportedly regulated by binding of β-catenin to T-cell-specific transcription factor 4 (TCF4)-binding sites(9). Human defensin 6 (HD6) is also a member of the α-defensin family and is expressed by Paneth cells(10). Because of poor antibacterial potency, the molecular mechanism underlying HD6 expression has yet not been assessed(11). However, HD6 has recently been reported to act as a mucosal barrier by forming "nanonets" to trap bacteria(12). Furthermore, reduced form of HD6 has been shown to have a bactericidal effect because HD6 expression is also important in the formation of the mucosal barrier(13). In this study, we aimed to elucidate the molecular mechanism underlying HD6

For Peer Review

expression and determine the potential role of HD6 in CD pathogenesis. We then investigated the mechanisms regulating HD6 transcriptional activity and expression contributing to decreased HD6 levels in non-inflamed jejunum of CD patients using mapping biopsies of the entire small intestine.

For Peer Review

Materials and Methods

Cell culture and chemicals

Human colon cancer-derived SW480 and DLD-1 cells were grown in Dulbecco's modified Eagle medium (Life Technologies, Grand Island, NY, USA) supplemented with 10% fetal bovine serum and 0.01% penicillin-streptomycin. Except where indicated otherwise, cells were seeded at a density of 5×10^5 cells/mL in each experiment. Cell cultures and plasmid DNA transfections were performed as previously described(14). 5μM Calphostin C (Sigma-Aldrich, St. Louis, MO, USA) was added to media to inhibit β-catenin/TCF4 complex formation(15).

Plasmids

An mCherry-Atoh1 vector was generated by inserting the *ATOH1* gene into the mCherry DNA template PG27188 (DNA 2.0, Menlo Park, CA, USA). An *ATOH1* gene mutant vector (5SA-Atoh1) was constructed by PCR-mediated mutagenesis by replacing nucleotide cording for five serine residues, TCC (160–162) and AGC (172–174, 328–330, 340–342, 352–354), with nucleotides coding for the alanine residue, GCC. The Atoh1-lentivirus vector was generated by inserting the PCR-amplified mCherry-Atoh1 or mCherry-5SA-Atoh1 plasmid into pLenti 6.4 (Invitrogen) as previously described(16). Lentiviruses were generated according to the procedure manual. A HD6 reporter plasmid was generated by cloning a 1000- and 241-bp sequence of the human HD6 gene, HD6, into a pGL4 basic vector (Promega, Madison, WI, USA). A mutant HD6 promoter was constructed using polymerase chain reaction (PCR)-mediated mutagenesis to delete TCF4-binding sites and E-box sites. The primer

For Peer Review

sequences used in this study are summarized in Supplementary Table S1.

Quantitative Real-time PCR

Total RNA was isolated using an RNeasy Micro Kit (QIAGEN), according to the manufacturer's instructions. One-microgram aliquots of total RNA were used for cDNA synthesis in 20 μl reaction volumes. One microliter of cDNA was amplified with SYBR-Green in 20 μl reactions as previously described(14). The primer sequences used in this study are summarized in Supplementary Table S1. The amount of mRNA expression was normalized by β-actin.

Luciferase Assays

SW480 cells were seeded in six-well plate culture dishes and transfected with 4 μg of reporter plasmid along with 10 ng of pRL-TK plasmid (Promega). Cells were harvested 36 h after transfection, lysed by three cycles of freezing and thawing, and the luciferase activities of each sample, measured in arbitrary units, were normalized against Renilla luciferase activities as previously described(14).

Chromatin Immunoprecipitation (ChIP) Assay

ChIP assays were performed as previously described with some modifications. DLD1 and DLD1-mCherry-Atoh1-5SA cells were seeded onto a 150-mm dish. Immunoprecipitation was performed overnight at 4°C with 10 μg of an anti-mCherry (Clontech, USA), normal mouse immunoglobulin G (sc-2025; Santa Cruz

For Peer Review

Biotechnology, Santa Cruz, CA, USA), or an anti-histone H3 antibody (Abcam, Cambridge, MA, USA). Genomic DNA fragments in immunoprecipitated samples were analyzed by PCR using primers designed against genomic DNA regions relative to the translation start site (Supplementary Table S1). Equal amounts of DNA samples were analyzed by conventional PCR in parallel using the following parameters: denaturation at 94°C for 15 s; annealing at 60°C for 30 s; and extension at 68°C for 60 s for 45 cycles. Products were resolved by agarose gel electrophoresis, stained with ethidium bromide, and visualized using an ImageQuant TL system (GE Healthcare, Milwaukee, WI, USA).

Human Small Intestinal Tissue

Human tissue specimens were obtained from 15 CD and 9 non-IBD patients with an indication to undergo double balloon endoscopy or single balloon endoscopy at Tokyo Medical and Dental University Hospital. Patient's information is shown in Supplementary Table S2. Non-IBD patients were performed endoscopy because of the obscure gastrointestinal bleeding. To analyze the structure of normal small intestine, we selected biopsy specimens from non-IBD patients who showed no abnormality in small intestine(17). Written informed consent was obtained from all included patients and this study was approved by the Ethics Committee of Tokyo Medical and Dental University.

Microarray analysis

For Peer Review

Total RNA was extracted using standard protocols (Affymetrix). Targets were prepared and hybridized to GeneChip Human Gene 1.0 ST arrays (Affymetrix), according to standard protocols. GeneChip data sets were analyzed using GeneSpring GX 7.3.1 (Agilent). Array data were normalized using robust multi-array analysis considering guanine and cytosine content algorithms (18). This result was assigned the GEO accession number GSE69762.

Immunohistochemistry

Immunohistochemical analysis of human small intestine was conducted using paraffin-embedded and frozen sections. Tissue sections were stained following microwave treatment (500W, 10 min) in 10 mM citrate buffer. An Atoh1 antibody, originally generated by immunizing rabbits with Atoh1 peptide, were used as previously described(17). Anti-HD6 (Atlas Antibodies) and anti-β-catenin (BD Biosciences) antibodies were also used. Primary antibodies were visualized using secondary antibodies conjugated to either Alexa-594 or Alexa-488 (Life Technologies). Sections were mounted using VectaShield mounting medium containing DAPI (Vector Laboratories) and visualized by confocal laser fluorescent microscopy (FLUOVIEW FV10i;Olympus) as previously described(19).

Statistical Analyses

Quantitative real-time PCR analyses were statistically analyzed using the Student's t-

For Peer Review

test. P-values <0.05 were considered statistically significant. In the cases of more than two data sets existed, differences between groups were determined using one-way analysis of variance (ANOVA) and Bonferroni's post hoc method of multiple comparisons.

For Peer Review

Results

Atoh1 upregulates HD6 expression and transcriptional activity

To assess the expression of Paneth cell phenotypic genes in response to Atoh1, we transiently transfected the *ATOH1* gene into SW480 cells, resulting in marked upregulation of HD6 only in response to Atoh1 (Fig. 1a). We therefore investigated the HD6 promoter region. As there are three TCF4-binding sites and four E-box-binding sites within 1000 bp of the HD6 promoter region (Fig. 1b), we constructed two reporter plasmids to assess HD6 transcriptional activity (Fig. 1c). Reporter analysis demonstrated significant upregulation of HD6 transcriptional activity by Atoh1 within 241 bp of the HD6 promoter region in addition to 1000 bp of the HD6 promoter region (Fig. 1d).

An E-box-binding site within the HD6 promoter is crucial for the transcriptional regulation by Atoh1

We then investigated the three TCF-binding sites within 1000 bp of the HD6 promoter region has previously been reported to be regulated by β-catenin via TCF-binding sites. Deletion mutation of the TCF-binding sites demonstrated the TCF-binding site at 178 bp (T3) was significantly affected transcriptional regulation of HD6 by Atoh1 (Fig. 2a). As Atoh1 recognizes and binds to the E-box sequence(20), we constructed E-box deletion mutants of HD6 reporter plasmids. Deletion mutation of the E-box-binding site demonstrated the E-box-binding site at 101 bp (E3) significantly affected transcriptional regulation of HD6 by Atoh1 (Fig. 2b). Deletion of both T3 and E3 resulted in significantly decreased HD6 transcriptional activity compared to individual deletions (Fig. 2c), indicating that E3 and T3 may be crucial for Atoh1-induced HD6 expression.

For Peer Review

Atoh1 directly binds to the HD6 promoter region

We next assessed whether Atoh1 directly binds to the HD6 promoter region. We generated stable DLD1 cell lines that strongly expressed Atoh1 protein as previously described (mCherry 5SA Atoh1)(16). We then designed primers for ChIP assays as shown in Fig. 3a. ChIP assays demonstrated the direct binding of Atoh1 within 200 bp of the HD6 promoter region (Fig. 3b).

β-catenin regulates HD6 expression in cooperation with Atoh1

As DLD1 and SW480 cells are generated from human colon cancer with APC gene deletions, nuclear accumulation of β-catenin protein is observed in these cells. The presence of β-catenin alone was not found to induce HD6 expression (Fig. 1a). We therefore assessed the effect of β-catenin on Atoh1-induced HD6 expression. Treatment with calphostin C, an inhibitor of the binding of β-catenin to TCF4, resulted in decreased levels of cyclin D1. Treatment of Atoh1-expressing cells with calphostin C led to decreased HD6 expression with no effect on TCF4 expression (Fig. 4a). Calphostin C also caused decreased Atoh1-induced HD6 transcriptional activity (Fig. 4b). Interestingly, calphostin C was shown to decrease transcriptional activity in response to the TCF4-binding site deletion mutant, indicating β-catenin may regulate HD6 expression via the E-box biding site (E3) in cooperation with Atoh1 (Fig. 4c).

Atoh1 protein colocalizes with β-catenin in HD6-expressing Paneth cells

We next assessed the localization of Atoh1 and β-catenin in human Paneth cells. β-catenin was found to be expressed in the nuclei of crypt base cells, whereas Atoh1 was

For Peer Review

expressed in the nuclei of almost all epithelial cells (Fig. 5a). Double immunostaining for HD6 and Atoh1 also demonstrated nuclear expression of Atoh1 in HD6-expressing cells (Fig. 5b). Double immunostaining for HD6 and β-catenin demonstrated nuclear accumulation of β-catenin in HD6-expressing cells demonstrating colocalization of Atoh1 and β-catenin in HD6 expressing Paneth cells (Fig. 5c). Moreover, double immunostaining for HD5 and β-catenin demonstrated nuclear accumulation of β-catenin in HD5-expressing cells demonstrating colocalization of Atoh1 and β-catenin in HD5 expressing Paneth cells (Fig. 5d). Furthermore, double immunostaining for HD5 and HD6 demonstrated that HD6 and HD5 were expressed in the same cells in almost Paneth cells (Supplementary Figure S1a). However, HD6 single positive cell was detected in some crypts (Supplementary Figure S1b).

The HD6 expression is decreased in non-inflamed jejunum of CD patients due to impaired nuclear accumulation of β-catenin

Finally, we assessed HD6 expression in biopsy specimens from CD patients. To exclude the effect of inflammation, we performed microarray analysis using biopsy specimens (Supplementary Table S3). No significant upregulation of inflammation-related genes were detected in jejunal tissue from CD patients compared to non-IBD patients, whereas numerous inflammation-related genes were increased in biopsies taken from throughout the ileum of CD patients, suggesting that the jejunal state might reflect CD pathogenesis of intestinal epithelial cells without mucosal damage by the inflammation. No significant difference in the number of Paneth cells per crypt was observed between jejunal biopsies from CD and non-IBD patients (Figs. 6a,b). Interestingly, immunostaining for HD6 demonstrated markedly decreased levels of HD6

For Peer Review

in jejunal samples from CD patients (Fig. 6c). The number of HD6-positive cells per crypt was decreased in jejunal biopsies from CD patients. There was no difference in the number of HD5-positive cells per crypt between jejunal samples from CD and non-IBD patients (Figs. 6d,e). HD6-expressing cells were found to be entirely absent in a proportion of crypts in jejunal samples from CD patients (Fig 6d). We therefore further assessed the mechanisms underlying the presence of 8 HD6-negative crypts in 6 CD patients. Immunostaining demonstrated nuclear accumulation of β-catenin was impaired in all HD6-negative crypts, whereas nuclear expression of Atoh1 was observed in all cells (Fig. 6f) (Supplementary Figure S2).

Discussion

This study demonstrated regulation of HD6 expression by the binding of Atoh1 to an E-box-binding site in cooperation with β-catenin binding to a TCF4-binding site and an E-box-binding site in the HD6 promoter region. We further demonstrated decreased levels of HD6 in non-inflamed jejunal biopsy samples from CD patients due to impaired nuclear localization of β-catenin, but not Atoh1.

Previous studies have suggested β-catenin might regulate the HD6 expression in a similar manner to HD5 as β-catenin has also been shown to bind to the HD6 promoter region(21). However, β-catenin has yet to be shown to promote HD6 expression. Although ATOH1 expression is crucial for differentiation toward secretary cell lineages, including Paneth cells(22), whether ATOH1 also regulates expression of Paneth phenotypic genes remains unknown. In the present study, we demonstrate for the first time that HD6 expression is directly regulated by Atoh1 in cooperation with β-catenin. We further identified critical sequences allowing binding of Atoh1 and β-catenin to the

For Peer Review

HD6 promoter region resulting in HD6 gene transcription. Treatment with calphostin C, a β-catenin inhibitor, completely inhibited the expression and transcriptional activity of HD6. Deletion of the TCF4-binding site partially blocked the transcriptional activity of HD6, indicating β-catenin might regulate HD6 transcriptional activity via E-box-binding site in cooperation with Atoh1, in addition to binding to the TCF4-binding site. The interaction between Atoh1 and β-catenin remains unclear with more detailed future studies required to fully elucidate their contribution to the regulation of HD6 expression in Paneth cells. Moreover, individual Paneth phenotypic genes encoding products, such as HD5, lysozyme, and sPLA2 may be independently regulated suggesting that Paneth cell subtypes may exist that maintain homeostasis throughout the entire small intestine.

Interestingly, expression of HD6, but not HD5, was decreased in non-inflamed jejunal biopsies from CD patients. We performed gene expression pattern analysis of the entire small intestine of non-IBD patients using biopsy specimens collected by balloon-assisted enteroscopy(17). In this study, we collected biopsy specimens from the entire small intestine of CD patients in order to compare gene expression to tissues obtained from non-IBD patients. Numerous inflammation-related genes were found to be significantly increased in the whole ileum of CD patients compared with samples taken from corresponding regions in non-IBD patients. In particular, inflammation-related genes were upregulated in the proximal ileum regardless of endoscopic and pathological findings. Jejunal non-inflamed mucosa was selected based on endoscopic, pathological, and molecular findings to assess the primary pathogenesis of CD. Microarray analysis of jejunal tissue from four CD patients demonstrated no upregulation of inflammation-related genes compared to non-IBD patients. Consequently, we able to demonstrate decreased numbers of HD6-positive cells, but not HD5-positive cells, without an

For Peer Review

inflammatory effect in CD patients. We found the nuclear accumulation of β-catenin was impaired in HD6-negative crypts suggesting HD6 expression was suppressed due to decreased β-catenin, but not Atoh1, activity while the number of Paneth cells remained constant. It has been reported that HD6 is secreted as an oxidized peptide from the bottom of crypts into an aerobic environment and can be spontaneously reduced upon reaching the reducing environment of the intestinal lumen(13). Therefore, mucosal barrier dysfunction may occur in CD patients despite normal pathological findings. This process may be particularly relevant in Japanese CD patients with genetic variants affecting mucosal barrier function, such as NOD2(23) and ATG16L1(24), as a fundamental mechanism underlying the pathogenesis of CD. It should be considered that CD treatments may affect non-inflamed mucosa. However, assessment of the mucosa prior to the onset of CD using a prospective study is not possible, as we believe non-inflamed jejunal mucosa mimics findings prior to CD onset. Large-scale studies that include Caucasian and Asian patients are required to confirm this hypothesis.

In this study, Atoh1 expression was not altered in jejunum mucosa without the effect of inflammation. It has however been reported that HD6 expression was reduced in inflamed ileum(25) with aberrant Notch signal activation(26). Because Atoh1 is directly suppressed by Hes1 via Notch signaling(14), Atoh1 might be decreased in inflamed ileum of CD patients, resulting in the reduced HD6 expression in corporation with the impairment of β-catenin. In future, more detailed analysis for Atoh1 expression in inflamed ileum is also required to understand the mucosal barrier dysregulation in entire small intestine of CD patients.

In conclusion, HD6 is required for the nuclear accumulation of both Atoh1 and β-catenin in Paneth cells. Decreased levels of nuclear β-catenin, but not Atoh1, induce

For Peer Review

decreased levels of HD6 without impairment of epithelial differentiation toward Paneth cells in CD. Further studies of non-inflamed mucosa may further elucidate the mechanisms underlying the pathogenesis of CD.

Disclosures: The authors disclose no conflict of interest.

For Peer Review

References

1. Kaser A, Zeissig S, Blumberg R. Inflammatory bowel disease. Annu Rev Immunol. 2010;28:573-621

2. Maloy KJ, Powrie F. Intestinal homeostasis and its breakdown in inflammatory bowel disease. Nature. 2011;474:298-306

3. Strober W, Watanabe T. NOD2, an intracellular innate immune sensor involved in host defense and Crohn's disease. Mucosal Immunol. 2011;4:484-495

4. Cadwell K, Liu JY, Brown SL, et al. A key role for autophagy and the autophagy gene Atg16l1 in mouse and human intestinal Paneth cells. Nature. 2008;456:259-263

5. Kaser A, Lee AH, Franke A, et al. XBP1 links ER stress to intestinal inflammation and confers genetic risk for human inflammatory bowel disease. Cell. 2008;134:743-756

6. Jager S, Stange EF, Wehkamp J. Inflammatory bowel disease: an impaired barrier disease. Langenbecks Arch Surg. 2013;398:1-12

7. Clevers HC, Bevins CL. Paneth cells: maestros of the small intestinal crypts. Annu Rev Physiol. 2013;75:289-311

8. Okamoto R, Tsuchiya K, Nemoto Y, et al. Requirement of Notch activation during regeneration of the intestinal epithelia. Am J Physiol Gastrointest Liver Physiol. 2009;296:G23-35

9. van Es JH, Jay P, Gregorieff A, et al. Wnt signalling induces maturation of Paneth cells in intestinal crypts. Nat Cell Biol. 2005;7:381-386

10. Jones DE, Bevins CL. Defensin-6 mRNA in human Paneth cells: implications for antimicrobial peptides in host defense of the human bowel. FEBS Lett.

For Peer Review

1993;315:187-192

11. Ericksen B, Wu Z, Lu W, et al. Antibacterial activity and specificity of the six human {alpha}-defensins. Antimicrob Agents Chemother. 2005;49:269-275

12. Chu H, Pazgier M, Jung G, et al. Human α-defensin 6 promotes mucosal innate immunity through self-assembled peptide nanonets. Science. 2012;337:477-481

13. Schroeder BO, Ehmann D, Precht JC, et al. Paneth cell alpha-defensin 6 (HD-6) is an antimicrobial peptide. Mucosal Immunol. 2015;8:661-671

14. Zheng X, Tsuchiya K, Okamoto R, et al. Suppression of hath1 gene expression directly regulated by hes1 via notch signaling is associated with goblet cell depletion in ulcerative colitis. Inflamm Bowel Dis. 2011

15. Lepourcelet M, Chen YN, France DS, et al. Small-molecule antagonists of the oncogenic Tcf/beta-catenin protein complex. Cancer Cell. 2004;5:91-102

16. Kano Y, Tsuchiya K, Zheng X, et al. The acquisition of malignant potential in colon cancer is regulated by the stabilization of Atonal homolog 1 protein. Biochem Biophys Res Commun. 2013;432:175-181

17. Iwasaki M, Tsuchiya K, Okamoto R, et al. Longitudinal cell formation in the entire human small intestine is correlated with the localization of Hath1 and Klf4. J Gastroenterol. 2011;46:191-202

18. Fukuda S, Toh H, Hase K, et al. Bifidobacteria can protect from enteropathogenic infection through production of acetate. Nature. 2011;469:543-547

19. Horita N, Tsuchiya K, Hayashi R, et al. Fluorescent labelling of intestinal epithelial cells reveals independent long-lived intestinal stem cells in a crypt. Biochem Biophys Res Commun. 2014;454:493-499

20. Akazawa C, Ishibashi M, Shimizu C, et al. A mammalian helix-loop-helix

For Peer Review

factor structurally related to the product of Drosophila proneural gene atonal is a positive transcriptional regulator expressed in the developing nervous system. J Biol Chem. 1995;270:8730-8738

21. Wehkamp J, Wang G, Kubler I, et al. The Paneth cell alpha-defensin deficiency of ileal Crohn's disease is linked to Wnt/Tcf-4. J Immunol. 2007;179:3109-3118

22. Yang Q, Bermingham N, Finegold M, et al. Requirement of Math1 for secretory cell lineage commitment in the mouse intestine. Science. 2001;294:2155-2158

23. Inoue N, Tamura K, Kinouchi Y, et al. Lack of common NOD2 variants in Japanese patients with Crohn's disease. Gastroenterology. 2002;123:86-91

24. Yamazaki K, Onouchi Y, Takazoe M, et al. Association analysis of genetic variants in IL23R, ATG16L1 and 5p13.1 loci with Crohn's disease in Japanese patients. J Hum Genet. 2007;52:575-583

25. Wehkamp J, Salzman NH, Porter E, et al. Reduced Paneth cell alpha-defensins in ileal Crohn's disease. Proc Natl Acad Sci U S A. 2005;102:18129-18134

26. Dahan S, Rabinowitz KM, Martin AP, et al. Notch-1 signaling regulates intestinal epithelial barrier function, through interaction with CD4+ T cells, in mice and humans. Gastroenterology. 2011;140:550-559

For Peer Review

Figure Legends

Figure 1. Atoh1 up regulates *HD6* expression and transcriptional activity

(a) mCherry-Atoh1 or GFP was transfected into SW480 cells. After 48 h, the expression of human AMPs was determined by RT-PCR. The amount of mRNA expression was normalized by β-actin. Statistical analysis was used Student's t-test. *p < 0.05, **p < 0.01, ***p < 0.001, n = 3. N.S.: not significant. (b) Schematic representation of the HD6 promoter region. There are three TCF4-binding sites (T/A-T/A-CAAAG) and four E-box-binding sites (CANNTG) within 1000 bp. (c) Schematic representation of HD6 reporter plasmids. We constructed two different lengths of the HD6 promoter region, 1000 bp and 241 bp, respectively. Each binding sites were numbered. (d) HD6 reporter activity of by Atoh1 was analyzed. Atoh1 significantly promoted the reporter activity of a 241-bp HD6 promoter region as well as a 1000-bp HD6 promoter region. Statistical analysis was used one-way analysis of variance (ANOVA) and Bonferroni's post hoc method. *p < 0.05, **p < 0.01, ***p < 0.001, n = 3. N.S.: not significant.

Figure 2. An E-box-binding site on HD6 promoter is crucial for the transcriptional activity by Atoh1

(a) All or each TCF4-binding sites within 1000 bp of the HD6 promoter region were deleted by mutagenesis. Each reporter plasmids were transfected with Atoh1 into SW480 cells. 48 h after transfection, reporter assay showed significant suppression of transcriptional activity in the T3 deletion mutant as well as that in the deletion mutant of all TCF4-binding sites. (b) All or each E-box-binding sites within 241 bp of the HD6

For Peer Review

promoter region were deleted by mutagenesis. Each reporter plasmids was transfected with Atoh1 into SW480 cells. Forty-eight hours after transfection, reporter assay showed significant suppression of transcriptional activity in the E3 deletion mutant, which was almost identical to that in the deletion mutant of all E-box-binding sites. Statistical analysis was used one-way analysis of variance (ANOVA) and Bonferroni's post hoc method. *p < 0.05, **p < 0.01, ***p < 0.001, n = 3. N.S.: not significant.

Figure 3. Atoh1 directly binds the HD6 promoter region

(a) ChIP assay was performed using DLD1 cells with or without mCherry 5SA-Atoh1. Each region is indicated by a schematic. (b) Each region was amplified from the immunoprecipitant by each antibody. Only the region including the 13–290-bp segment of the HD6 promoter (region b) was amplified from the immunoprecipitant by the mCherry antibody. H3: anti-histone 3 antibody was used as positive control.

Figure 4. β-catenin also regulates the HD6 expression in cooperation with Atoh1

(a) β-catenin inhibitors were transfected into mCherry 5SA-Atoh1 DLD1 cells for 48 h. The expression of each gene was analyzed by RT-PCR. The amount of mRNA expression was normalized by β-actin. Statistical analysis was used Student's t-test. *p < 0.05, **p < 0.01, ***p < 0.001, n = 3. N.S.: not significant. (b, c) Each reporter plasmid was transfected into mCherry 5SA-Atoh1 DLD1 cells with either DMSO or β-catenin inhibitor. Forty-eight hours after transfection, the reporter activity was assessed. Statistical analysis was used one-way analysis of variance (ANOVA) and Bonferroni's post hoc method. *p < 0.05, **p < 0.01, ***p < 0.001, n = 3. N.S.: not significant.

For Peer Review

Figure 5. Atoh1 protein is colocalized with β-catenin in HD6-expressing Paneth cells

(a) Immunofluorescence double-staining of Atoh1 and β-catenin in human intestine of non-IBD patients merged with DAPI showed colocalization of Atoh1 and β-catenin in nuclei (arrow head). Scale bar, 10 μm. (b) Immunofluorescence double-staining of HD6 and Atoh1 in human intestine of non-IBD patients merged with DAPI showed nuclear expression of Atoh1 in HD6-expressing cells. Scale bar, 10 μm. (c) Immunofluorescence double-staining of HD6 and β-catenin in human intestine of non-IBD patients merged with DAPI showed nuclear accumulation of β-catenin in HD6-expressing cells (arrow head). Scale bar, 10 μm. (d) Immunofluorescence double-staining of HD5 and β-catenin in human intestine of non-IBD patients merged with DAPI showed nuclear accumulation of β-catenin in HD5-expressing cells (arrow head). Scale bar, 10 μm.

Figure 6. HD6 expression decreased in non-inflamed jejunum of CD patients due to impairing the nuclear accumulation of β-catenin

(a) HE-staining of jejunal specimen taken from CD patients or healthy control. Paneth cells are located at the base of crypt shown as a cell with large eosinophilic refractile granules in cytoplasm. Scale bar, 10 μm. (b) The average number of Paneth cells per a crypt in the CD or non-IBD patients. The number of Paneth cells was counted at over 10 crypts/person. (c) Immunofluorescence analysis of HD6 merged with DAPI in non-inflamed jejunum of CD or non-IBD patients. Scale bar, left panel; 500 μm, right panel; 10 μm. (d) The number of HD5- or HD6-positive cells per crypt in the CD or non-IBD

For Peer Review

patients. The positive crypt of HD5 was investigated in 213 crypts of 9 non-IBD patients and 377 crypts of 15 CD patients, respectively. The positive crypt of HD6 was investigated in 248 crypts of 9 non-IBD patients and 391 crypts of 15 CD patients, respectively. (e) The average number of HD5- or HD6- positive cells per crypt in the CD or non-IBD patients. The number of Paneth cells was counted at over 10 crypts/person. (f) Immunofluorescence analysis of HD6 either with β-catenin or Atoh1 merged with DAPI in non-inflamed jejunum of CD patients. Nuclear accumulation of β-catenin was impaired in all HD6 negative crypts. Scale bar, 10 μm. Atoh1 expression was not changed despite HD6 expression. Arrow heads point to HD6 positive cells. Statistical analysis was used Student's t-test. **$p < 0.01$, ***$p < 0.001$. N.S.: not significant.

For Peer Review

Figure 1

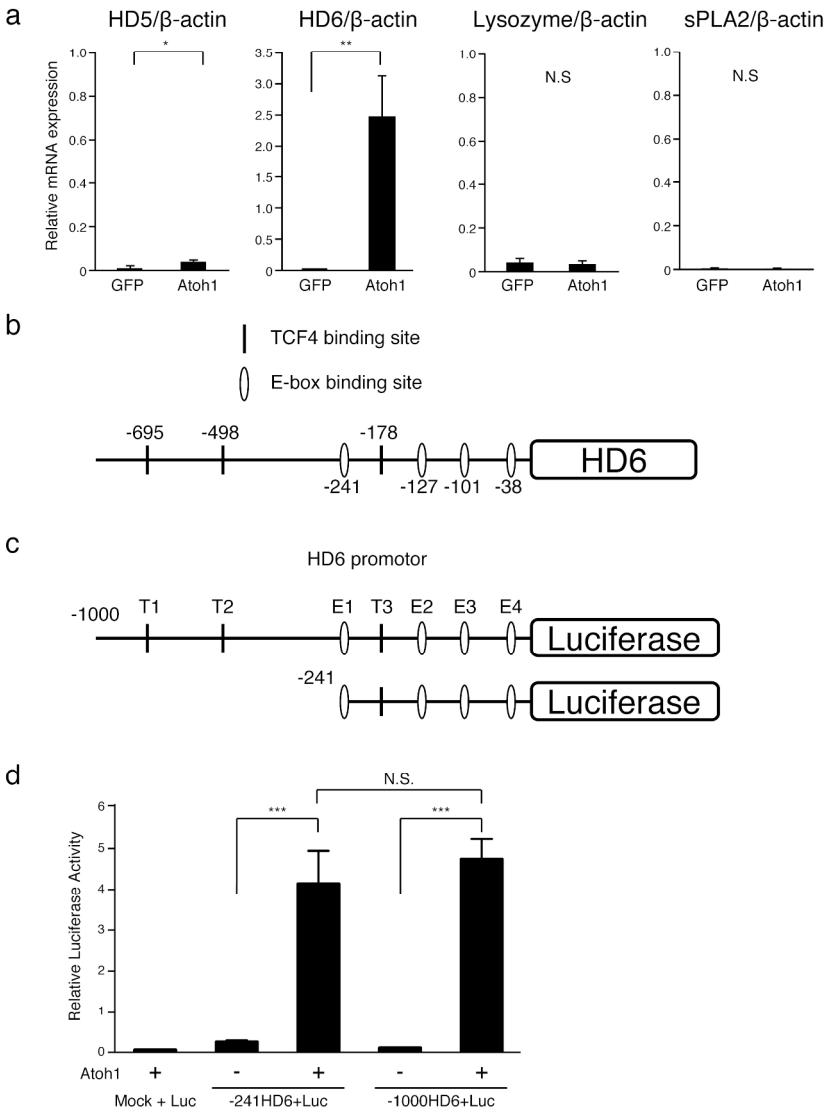

Figure 1. Atoh1 up regulates HD6 expression and transcriptional activity
(a) mCherry-Atoh1 or GFP was transfected into SW480 cells. After 48 h, the expression of human AMPs was determined by RT-PCR. The amount of mRNA expression was normalized by β-actin. Statistical analysis was used Student's t-test. *p < 0.05, **p < 0.01, ***p < 0.001, n = 3. N.S.: not significant. (b) Schematic representation of the HD6 promoter region. There are three TCF4-binding sites (T/A-T/A-CAAAG) and four E-box-binding sites (CANNTG) within 1000 bp. (c) Schematic representation of HD6 reporter plasmids. We constructed two different lengths of the HD6 promoter region, 1000 bp and 241 bp, respectively. Each binding sites were numbered. (d) HD6 reporter activity of by Atoh1 was analyzed. Atoh1 significantly promoted the reporter activity of a 241-bp HD6 promoter region as well as a 1000-bp HD6 promoter region. Statistical analysis was used one-way analysis of variance (ANOVA) and Bonferroni's post hoc method. *p < 0.05, **p < 0.01, ***p < 0.001, n = 3. N.S.: not significant.
190x266mm (300 x 300 DPI)

For Peer Review

Figure 2

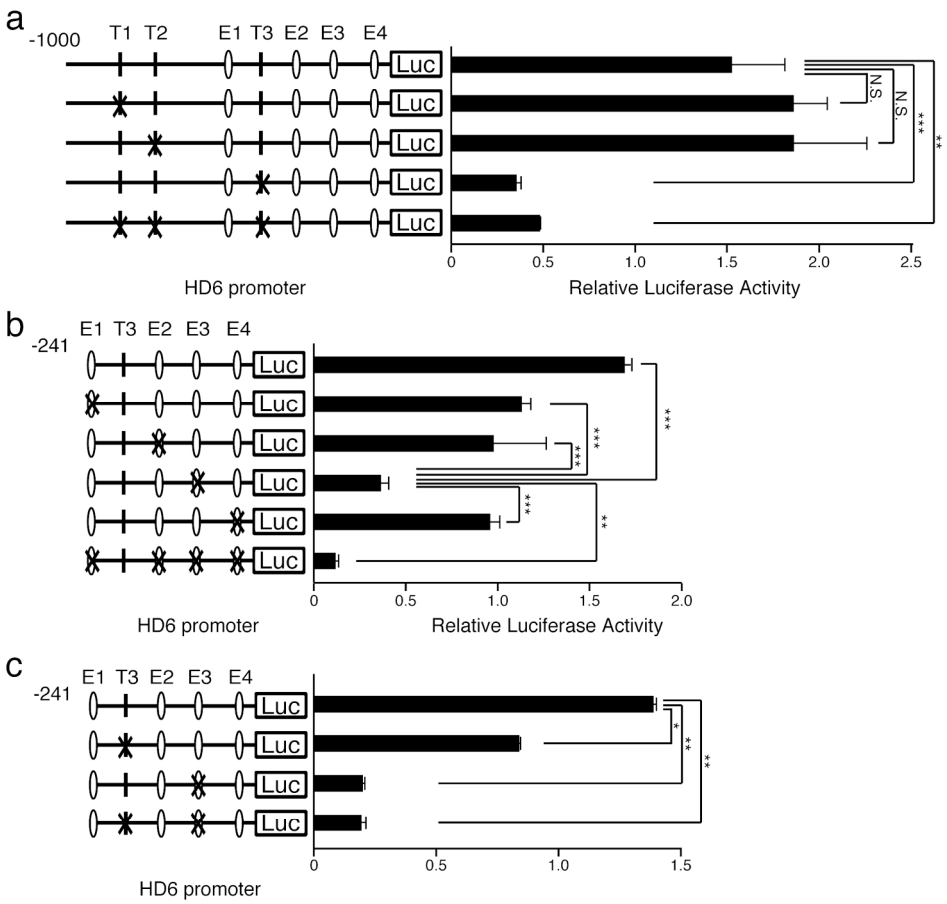

Figure 2. An E-box-binding site on HD6 promoter is crucial for the transcriptional activity by Atoh1
(a) All or each TCF4-binding sites within 1000 bp of the HD6 promoter region were deleted by mutagenesis. Each reporter plasmids were transfected with Atoh1 into SW480 cells. 48 h after transfection, reporter assay showed significant suppression of transcriptional activity in the T3 deletion mutant as well as that in the deletion mutant of all TCF4-binding sites. (b) All or each E-box-binding sites within 241 bp of the HD6 promoter region were deleted by mutagenesis. Each reporter plasmids was transfected with Atoh1 into SW480 cells. Forty-eight hours after transfection, reporter assay showed significant suppression of transcriptional activity in the E3 deletion mutant, which was almost identical to that in the deletion mutant of all E-box-binding sites. Statistical analysis was used one-way analysis of variance (ANOVA) and Bonferroni's post hoc method. *p < 0.05, **p < 0.01, ***p < 0.001, n = 3. N.S.: not significant.
181x189mm (300 x 300 DPI)

Figure 3

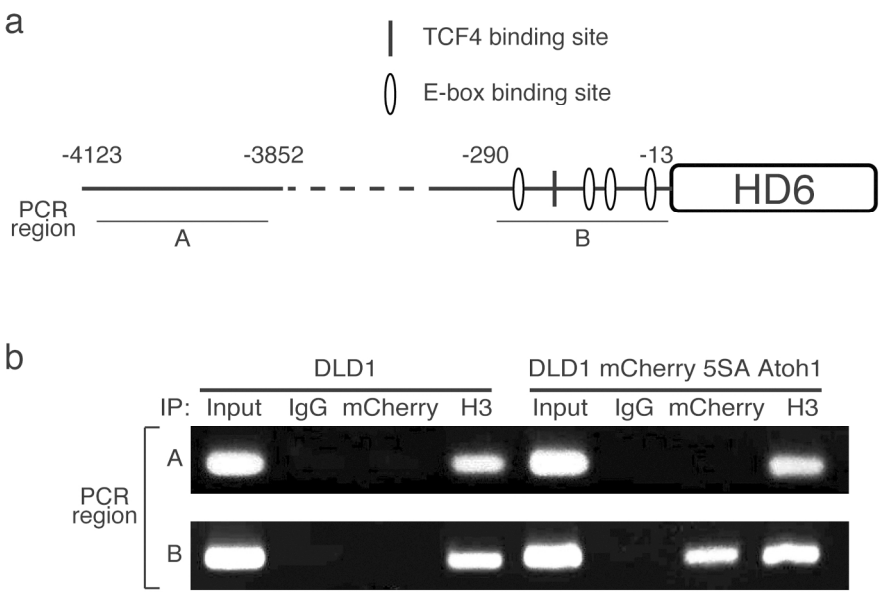

Figure 3. Atoh1 directly binds the HD6 promoter region
(a) ChIP assay was performed using DLD1 cells with or without mCherry 5SA-Atoh1. Each region is indicated by a schematic. (b) Each region was amplified from the immunoprecipitant by each antibody. Only the region including the 13–290-bp segment of the HD6 promoter (region b) was amplified from the immunoprecipitant by the mCherry antibody. H3: anti-histone 3 antibody was used as positive control.
178x133mm (300 x 300 DPI)

For Peer Review

Figure 4

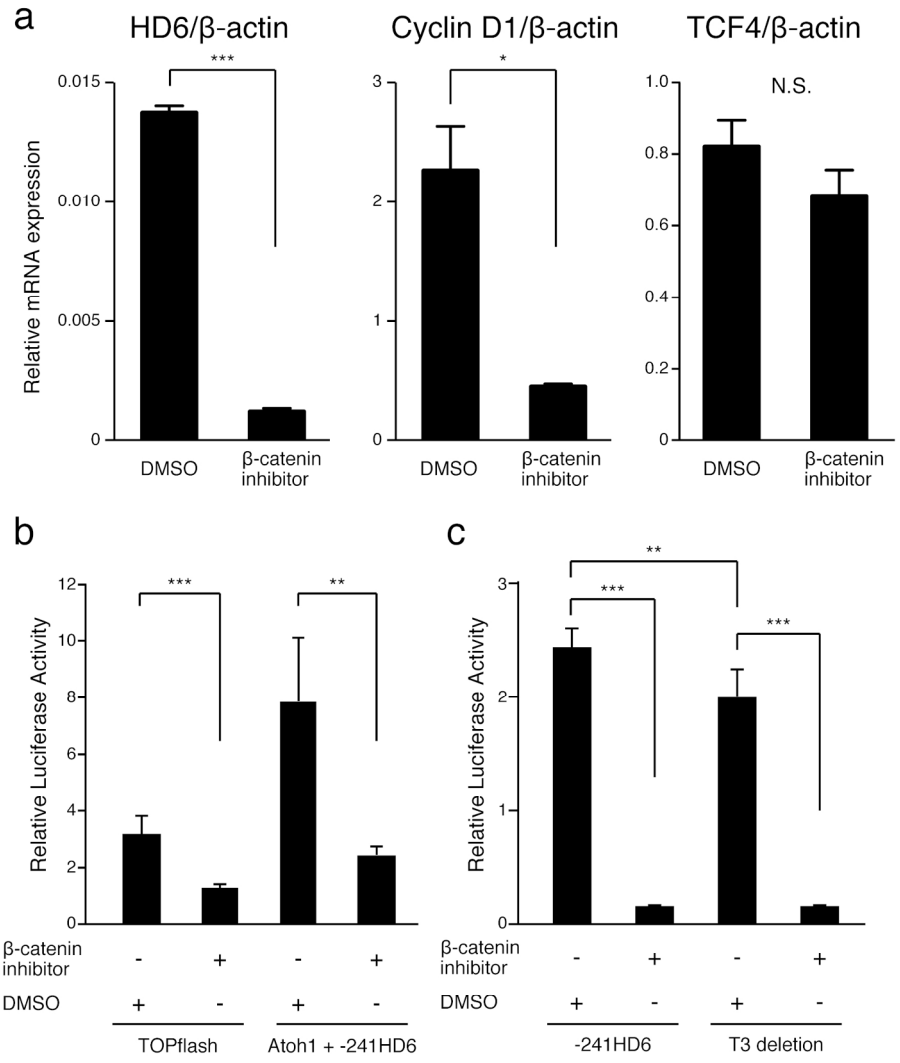

Figure 4. β-catenin also regulates the HD6 expression in cooperation with Atoh1
(a) β-catenin inhibitors were transfected into mCherry 5SA-Atoh1 DLD1 cells for 48 h. The expression of each gene was analyzed by RT-PCR. The amount of mRNA expression was normalized by β-actin. Statistical analysis was used Student's t-test. *p < 0.05, **p < 0.01, ***p < 0.001, n = 3. N.S.: not significant. (b, c) Each reporter plasmid was transfected into mCherry 5SA-Atoh1 DLD1 cells with either DMSO or β-catenin inhibitor. Forty-eight hours after transfection, the reporter activity was assessed. Statistical analysis was used one-way analysis of variance (ANOVA) and Bonferroni's post hoc method. *p < 0.05, **p < 0.01, ***p < 0.001, n = 3. N.S.: not significant.
165x198mm (300 x 300 DPI)

Figure 5

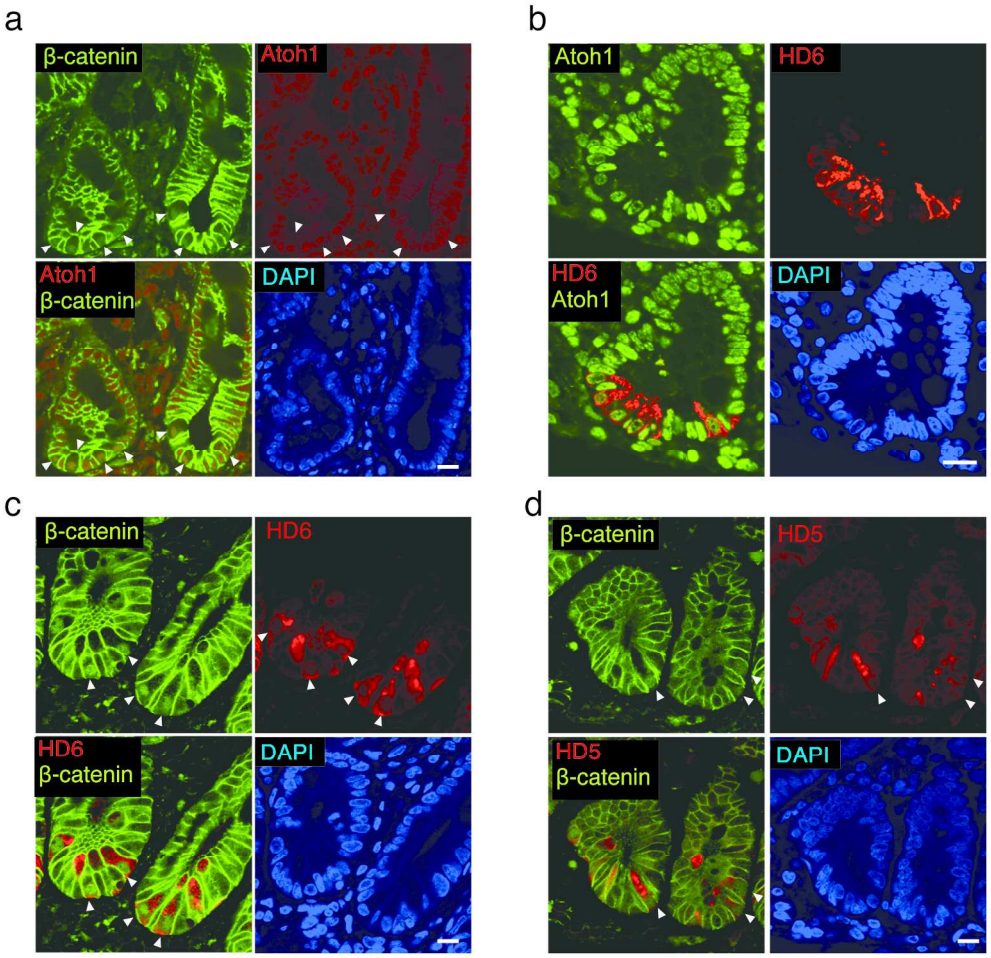

Figure 5. Atoh1 protein is colocalized with β-catenin in HD6-expressing Paneth cells
(a) Immunofluorescence double-staining of Atoh1 and β-catenin in human intestine of non-IBD patients merged with DAPI showed colocalization of Atoh1 and β-catenin in nuclei (arrow head). Scale bar, 10 μm. (b) Immunofluorescence double-staining of HD6 and Atoh1 in human intestine of non-IBD patients merged with DAPI showed nuclear expression of Atoh1 in HD6-expressing cells. Scale bar, 10 μm. (c) Immunofluorescence double-staining of HD6 and β-catenin in human intestine of non-IBD patients merged with DAPI showed nuclear accumulation of β-catenin in HD6-expressing cells (arrow head). Scale bar, 10 μm. (d) Immunofluorescence double-staining of HD5 and β-catenin in human intestine of non-IBD patients merged with DAPI showed nuclear accumulation of β-catenin in HD5-expressing cells (arrow head). Scale bar, 10 μm.
185x187mm (300 x 300 DPI)

Figure 6

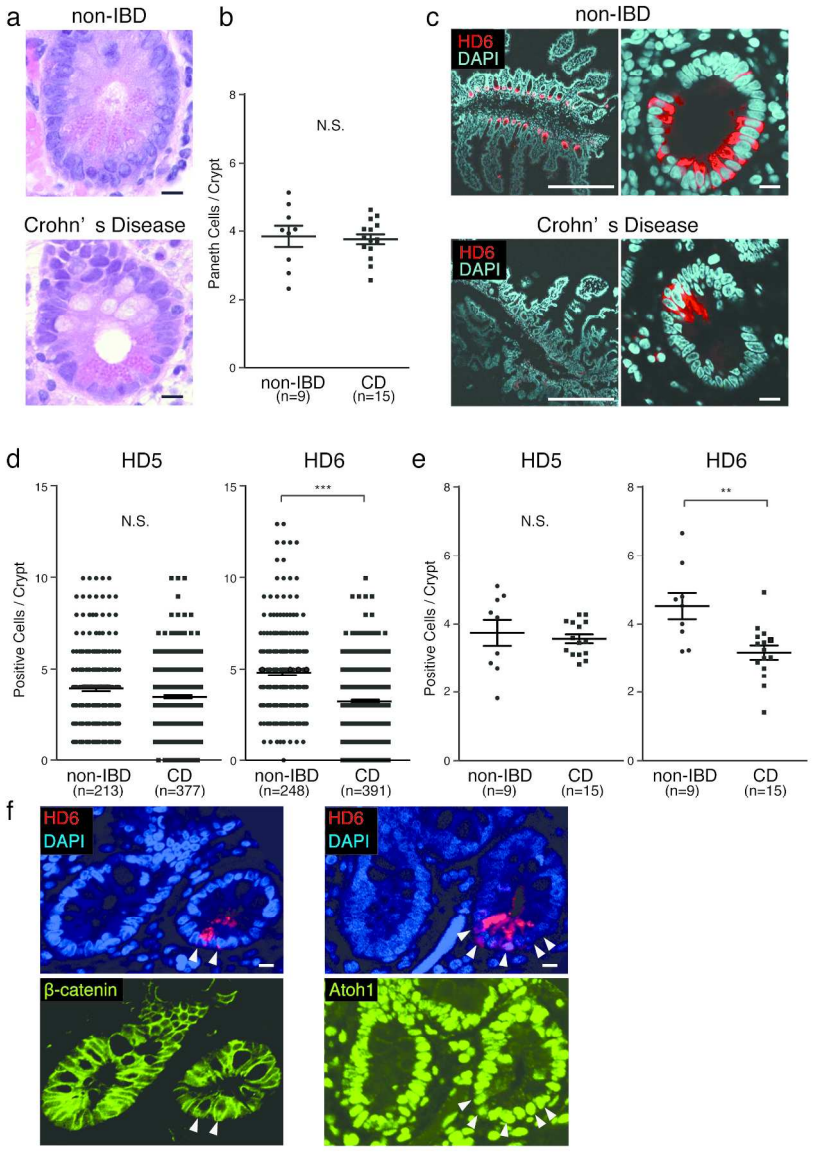

Figure 6. HD6 expression decreased in non-inflamed jejunum of CD patients due to impairing the nuclear accumulation of β-catenin

(a) HE-staining of jejunal specimen taken from CD patients or healthy control. Paneth cells are located at the base of crypt shown as a cell with large eosinophilic refractile granules in cytoplasm. Scale bar, 10 μm. (b) The average number of Paneth cells per a crypt in the CD or non-IBD patients. The number of Paneth cells was counted at over 10 crypts/person. (c) Immunofluorescence analysis of HD6 merged with DAPI in non-inflamed jejunum of CD or non-IBD patients. Scale bar, left panel; 500 μm, right panel; 10 μm. (d) The number of HD5- or HD6-positive cells per crypt in the CD or non-IBD patients. The positive crypt of HD5 was investigated in 213 crypts of 9 non-IBD patients and 377 crypts of 15 CD patients, respectively. The positive crypt of HD6 was investigated in 248 crypts of 9 non-IBD patients and 391 crypts of 15 CD patients, respectively. (e) The average number of HD5- or HD6- positive cells per crypt in the CD or non-IBD patients. The number of Paneth cells was counted at over 10 crypts/person. (f) Immunofluorescence analysis of HD6 either with β-catenin or Atoh1 merged with DAPI in non-inflamed jejunum of CD patients.

Nuclear accumulation of β-catenin was impaired in all HD6 negative crypts. Scale bar, 10 μm. Atoh1 expression was not changed despite HD6 expression. Arrow heads point to HD6 positive cells. Statistical analysis was used Student's t-test. **p < 0.01, ***p < 0.001. N.S.: not significant.
197x286mm (300 x 300 DPI)

For Peer Review

Supplementary Figure S1

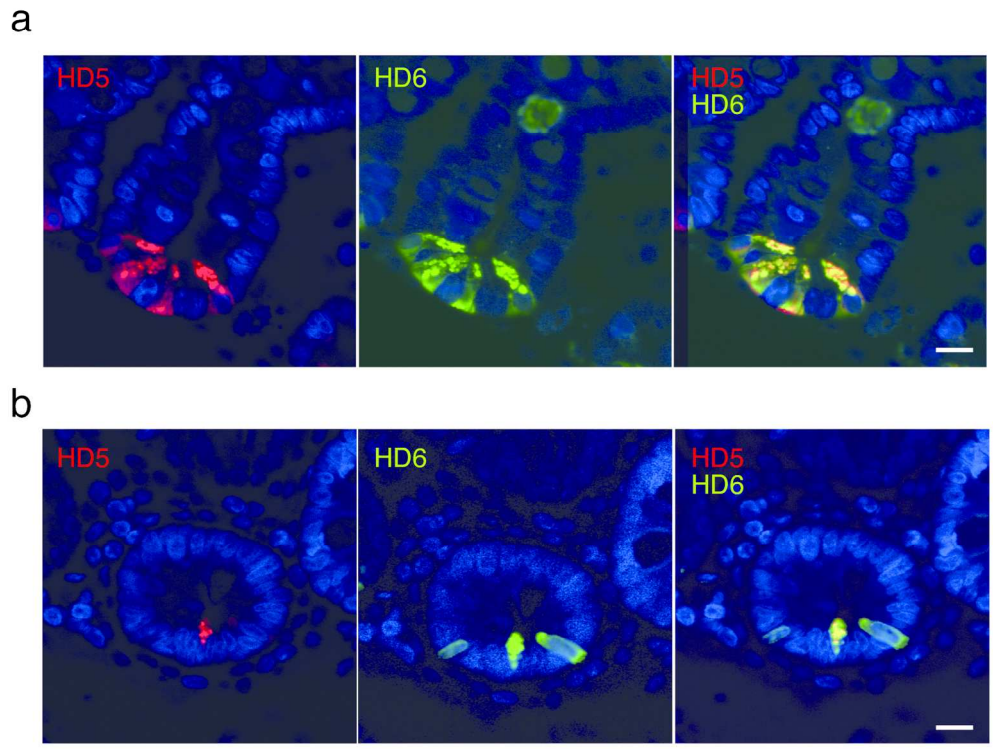

Supplementary Figure S1
(a) Immunofluorescence double-staining of HD5 and HD6 in human intestine of non-IBD patients merged with DAPI showed co-localization of HD5 and HD6. Scale bar, 10 μm.
(b) In some crypts, HD6 single positive cells were shown. Scale bar, 10 μm.
159x131mm (300 x 300 DPI)

Supplementary Figure S2

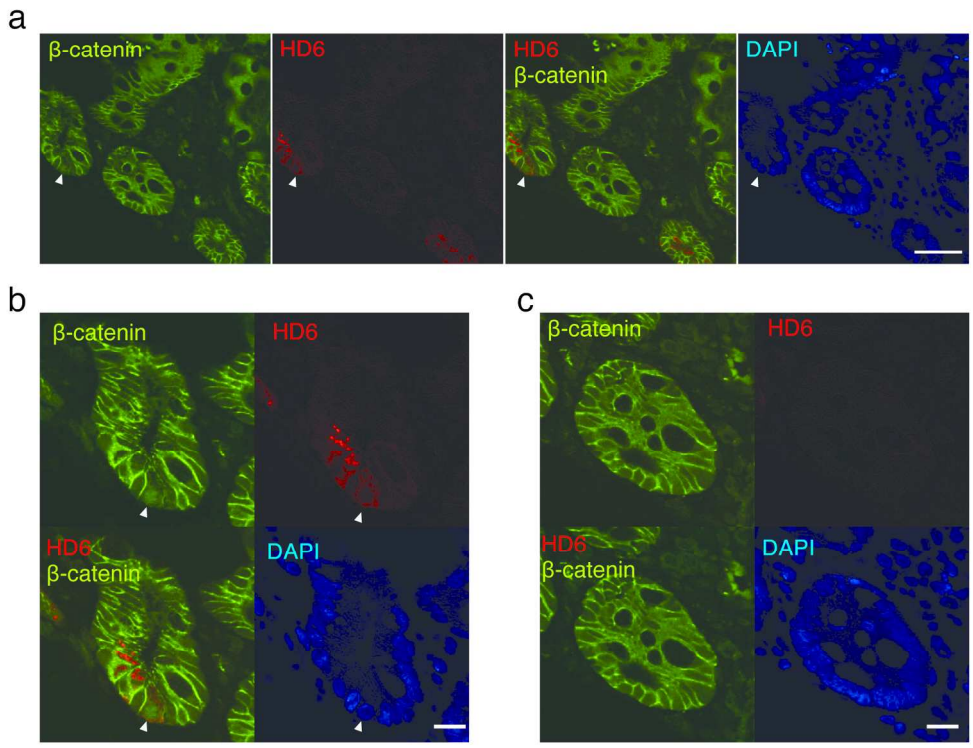

Supplementary Figure S2
(a) Immunofluorescence analysis of HD6 either with β-catenin merged with DAPI in non-inflamed jejunum of the other CD patient to Figure 6f. Nuclear accumulation of β-catenin was impaired only in HD6 negative crypt. Scale bar, 50 μm.
(b) High magnification image of HD6 positive crypt. Nuclear accumulation of β-catenin was shown in HD6 positive cell (arrow head). Scale bar, 10 μm.
(c) High magnification image of HD6 negative crypt. The nuclear localization of β-catenin is not shown in all cells. Scale bar, 10 μm.
186x148mm (300 x 300 DPI)

Hayashi et al. Supplementary Table S1

Quantitative analysis

Gene	Primer Sequence	
	Forward	Reverse
HD5	5' GCCATCCTTGCTGCCATTC 3'	5' TGATTTCACACACCCCGGAGA 3'
HD6	5' CCTCACCATCCTCACTGCTGTTC 3'	5' CCATGACAGTGCAGGTCCCATA 3'
Lysozyme	5' CTCTCATTGTTCTGGGGC 3'	5' ACGGACAACCCTCTTTGC 3'
PLA2G2A	5' ACCATGAAGACCCTCCTACTG 3'	5' GAAGAGGGGACTCAGCAACG 3'
cyclin D1	5' AGGCTGGTGGCAAGTGCACG 3'	5' TGTTGGTGCTGGGAAGCGCC 3'
TCF4	5' ATCGTCCCAGAGTGATGTCG 3'	5' CGGGCCAGCTCGTAGTATTT 3'
β -actin	5' GGATGCAGAAGGAGATCACTG 3'	5' CGATCCACACGGAGTACTTG 3'

Construction of HD6 Promoter

Gene	Primer Sequence	
	Forward	Reverse
HD6 (T1 del)	5'GTCAATTGTTTCGATGTTTTGGAGAGAAATACCTAGTAC3'	5'GTACTAGGTATTTCTCTCCAAAACATCGAAACAATTGAC3'
HD6 (T2 del)	5'CAAGAGCCTATTCACCCCATAATCCTCCTTCATGAGGGC3'	5'GCCCTCATGAAGGAGGATTATGGGGTGAATAGGCTCTTG3'
HD6 (T3 del)	5'TCACACTACAATGAAGCTTGGAGAAGGGACATGGAGGGCA3'	5'TGCCCTCCATGTCCCTTCTCCAAGCTTCATTGTAGTGTGA3'
HD6 (E1 del)	5' CGGGGTACCGGACCAGAACAGACACTCAAT 3'	5' AGTCAGTCAGCGAGAGCAGGAGCAGA 3'
HD6 (E2 del)	5'CCCAATCACACACTCCCCGTCTCACCGCAACATCTGTCCC3'	5'GGGACAGATGTTGCGGTGAGACGGGGAGTGTGTGATTGGG3'
HD6 (E3 del)	5'TCACATGCACTCCCCGTCTCACCGCAACATCTCCCTGAGCCTTC3'	5'GAAGGCTCAGGGAGATGTTGCGGTGAGACGGGGAGTGCATGTGA3'
HD6 (E4 del)	5'CTGGCTCCTCACTCCCCTCTGCTCCTGCTCTCTCTCCTC 3'	5'GAGGAGAGAGAGCAGGAGCAGAGGGGAGTGAGGAGCCAG3'
HD6 Kpn1 1000	5' AGTCAGTCGGTACCTGGACCCTTCTCTTT 3'	
HD6 kpn1 200	5' CGGGGTACCCAGCTGGGACCAGAACAGACA 3'	
3' Nhe Ⅰ HD6	5' AGTCAGTCAGCGAGAGCAGGAGCAGA 3'	

For Peer Review

ChiP assay

	Primer Sequence	
gene	Forward	Reverse
HD6 (-4123 -3852)	5' CCATCCAAGACGGTGAAAGT 3’	5’ TGGTCCCAATTCTTGGACTC 3’
HD6 (-290 -13)	5' CCAGCAGATGGAAAACAGGA 3’	5’ TGGAGGAGAGAGAGCAGGAG 3’

For Peer Review

Hayashi et al. Supplementary Table S2

	non-IBD (n=9)	Crohn's Disease (n=15)
Mean Age (y.o.) (range)	60.8 (37-80)	29.5 (19-60)
Gender		
Male	5 (55.6%)	13 (86.7%)
Female	4 (44.4%)	2 (13.3%)
Location of disease		
Ileitis		2 (13.3%)
Colitis		0 (0%)
Ileocolitis		13 (86.7%)
Treatment		
Anti-TNFα therapy		7 (46.7%)
Immunomodulator		7 (46.7%)
Steroid		0 (0%)
5-ASA		10 (66.7%)

Supplementary Table S2 legend

Patient's information in this study. Non-IBD patients were performed balloon endoscopy because of the obscure gastrointestinal bleeding. To analyze the structure of normal small intestine, we selected non-IBD patients who showed no abnormality in small intestine by balloon endoscopy.

For Peer Review

Hayashi et al. Supplementary Table S3

Jejunum UP

Identifiler	Gene title	Fold Change	p
NM_012128	CLCA4	3.2	0.06
NM_014080	DUOX2	3.0	0.07
NM_001040442	FABP6	2.6	0.14
NM_197975	BTNL3	2.5	0.09
NM_006890	CEACAM7	2.4	0.16
NR_006880|NR_003271	SNORD3A|SNORD3B-1	2.2	0.00002
|NR_003924|NR_006881|NR_006882	|SNORD3B-2|SNORD3C|SNORD3D		
NR_006880|NR_003271	SNORD3A|SNORD3B-1	2.2	0.00002
|NR_003924|NR_006881|NR_006882	|SNORD3B-2|SNORD3C|SNORD3D		
NR_006880|NR_003271	SNORD3A|SNORD3B-1	2.2	0.00003
|NR_003924|NR_006881|NR_006882	|SNORD3B-2|SNORD3C|SNORD3D		
NR_006880|NR_003271	SNORD3A|SNORD3B-1	2.2	0.00002
|NR_003924|NR_006881|NR_006882	|SNORD3B-2|SNORD3C|SNORD3D		
NR_006880|NR_003271	SNORD3A|SNORD3B-1	2.2	0.00003
|NR_003924|NR_006881|NR_006882	|SNORD3B-2|SNORD3C|SNORD3D		
NM_004591|NM_001130046	CCL20	2.2	0.03
NM_005564	LCN2	2.1	0.09
NM_002964	S100A8	2.1	0.08
NM_001018016	MUC1	2.1	0.13
NM_001828	CLC	2.0	0.005

For Peer Review

Jejunum DOWN

Identifiler	Gene title	Fold change	p
NM_001076|NM_001077	UGT2B15|UGT2B17	-5.6	0.009
NM_001076|NM_001077	UGT2B15|UGT2B17	-5.6	0.009
NM_001807	CEL	-5.6	0.06
NM_001077	UGT2B17	-3.6	0.007
NM_017460	CYP3A4	-2.9	0.11
NM_001074	UGT2B7	-2.8	0.002
NM_004617	TM4SF4	-2.5	0.10
NM_002021	FMO1	-2.5	0.08
NM_000771	CYP2C9	-2.5	0.02
NM_000040	APOC3	-2.5	0.04
NM_080669|NM_015077	SLC46A1|SARM1|TMEM199	-2.4	0.06
NM_000039	APOA1	-2.4	0.008
NM_000040	APOC3	-2.4	0.05
NM_000039	APOA1	-2.4	0.09
NM_000769	CYP2C19	-2.4	0.006
NM_080429	AQP10	-2.4	0.06
NM_002555	SLC22A18	-2.3	0.002
NM_019893|NM_001079516|XM_927086	ASAH2|ASAH2B|ASAH2C	-2.3	0.05
NM_019893|NM_001079516|XM_927086	ASAH2|ASAH2B|ASAH2C	-2.3	0.08
NM_001081	CUBN	-2.3	0.14
NM_003167	SULT2A1	-2.3	0.06
NM_020716	GRAMD1B	-2.2	0.03
NM_001045	SLC6A4	-2.2	0.05
NM_006424	SLC34A2	-2.2	0.01
NM_001001548	CD36	-2.2	0.04
NM_007180	TREH	-2.1	0.07
NM_006159	NELL2	-2.1	0.03
NM_022444	SLC13A1	-2.1	0.13
NM_000482	APOA4	-2.1	0.02
NM_019893|NM_001079516|XM_927086	ASAH2|ASAH2B|ASAH2C	-2.1	0.07
NM_019601	SUSD2	-2.1	0.05
NM_001003954	ANXA13	-2.1	0.02
NM_000482	APOA4	-2.1	0.13
NM_002299	LCT	-2.1	0.14
NM_004212	SLC28A2	-2.1	0.007
NM_000384	APOB	-2.1	0.22
NM_002242	KCNJ13	-2.0	0.19

For Peer Review

NM_145176	SLC2A12	-2.0	0.07
NM_005518	HMGCS2	-2.0	0.11
NM_000340	SLC2A2	-2.0	0.07

For Peer Review

Ileum UP

Identifiler	Gene title	Fold change	p
NM_004476	FOLH1	7.5	0.02
	LOC652493	5.7	0.02
	IGKV3D-11	4.6	0.04
	VSIG6	4.4	0.01
XM_002345544	IGKV3D-15|IGKV3-20|IGKV3D-11	4.3	0.04
	VSIG6|IGHA2|IGHG1	3.9	0.01
	HLA-DQB1	3.8	0.0001
	HLA-DQB1	3.8	0.00008
NM_000064	C3	3.6	0.03
	IGKC	3.6	0.03
NM_002123|NM_002124	HLA-DQB1|HLA-DRB1	3.5	0.005
NM_180991	SLCO4C1	3.4	0.05
NM_001778	CD48	3.4	0.03
	IGHV4-31|IGHA2|IGHA1|IGHG3 |IGHD |IGHM|IGHG1|IGHG2|IGHG4|IGHV3-23	3.4	0.03
NM_000063	C2	3.3	0.00006
NM_000063	C2	3.3	0.00008
NM_000063	C2	3.3	0.00007
	IGKC	3.3	0.05
NM_000560	CD53	3.3	0.04
NM_021814	ELOVL5	3.2	0.04
NM_021181	SLAMF7	3.2	0.05
	IGKC	3.2	0.04
NM_002122	HLA-DQA1	3.1	0.0004
	IGKC	3.1	0.03
NM_002185	IL7R	3.1	0.03
	IGHA1	3.0	0.03
	HLA-DQB1	3.0	0.0001
	LOC100291056	3.0	0.04
NM_001774	CD37	3.0	0.04
NM_002121	HLA-DPB1	3.0	0.01
NM_148672	CCL28	2.9	0.002
NM_006573	TNFSF13B	2.9	0.04
NM_033554	HLA-DPA1	2.8	0.02
NM_033554	HLA-DPA1	2.8	0.02
NM_033554	HLA-DPA1	2.8	0.01
	PTPRC	2.8	0.04

For Peer Review

NM_052931	SLAMF6	2.7	0.01
NM_002121	HLA-DPB1	2.7	0.01
NM_052941	GBP4	2.7	0.04
NM_007074	CORO1A	2.7	0.03
NM_001242	CD27	2.6	0.03
NM_002615	SERPINF1	2.6	0.03
NM_007293|NM_001002029	C4A|C4B	2.6	0.04
NM_007293|NM_001002029	C4A|C4B	2.6	0.04
NM_007293|NM_001002029	C4A|C4B	2.6	0.04
NM_002121	HLA-DPB1	2.6	0.00
NM_002738	PRKCB	2.6	0.04
	IGHA1	2.5	0.05
NM_002298	LCP1	2.5	0.05
	IGHM	2.5	0.04
NM_001465	FYB	2.5	0.05
NM_145799	SEPT6	2.5	0.02
NM_002872	RAC2	2.5	0.03
	IGKC|IGKV3D-15	2.5	0.03
NM_004862	LITAF	2.4	0.04
NM_006762	LAPTM5	2.4	0.05
NM_003650	CST7	2.4	0.05
NM_004536	NAIP	2.4	0.05
	IGKC	2.4	0.05
	LOC100293211	2.3	0.05
NM_031419	NFKBIZ	2.3	0.04
NM_002209	ITGAL	2.3	0.03
NM_004536	NAIP	2.3	0.05
NM_004536	NAIP	2.3	0.05
NM_004310	RHOH	2.3	0.04
	IGLJ3|IGHV3-23|IGHG1	2.3	0.04
NM_002120	HLA-DOB|TAP2	2.3	0.05
NM_001155	ANXA6	2.3	0.01
NM_001628	AKR1B1	2.3	0.03
NM_001130080	IFI27	2.2	0.002
NM_018326	GIMAP4	2.2	0.03
	IGHA1|IGHG1	2.2	0.04
NM_006674	HCP5	2.2	0.0002
NM_020056|NM_002122	HLA-DQA2|HLA-DQA1	2.2	0.01
NM_002120	HLA-DOB|TAP2	2.2	0.05
	IGHD|IGHG1|	2.2	0.04

For Peer Review

NM_020056|NM_002122	HLA-DQA2|HLA-DQA1	2.1	0.01
NM_001098526	AMICA1	2.1	0.02
NM_000310	PPT1	2.1	0.01
NM_000204	CFI	2.1	0.02
NM_014800	ELMO1	2.1	0.05
NM_181671	PITPNC1	2.1	0.03
NR_003937	HLA-DQB2	2.1	0.003
NM_004811	LPXN	2.1	0.02
NM_000732	CD3D	2.1	0.04
NM_000073	CD3G	2.1	0.04
NR_003937	HLA-DQB2	2.1	0.01
NM_005063	SCD	2.1	0.02
NM_001003927	EVI2A	2.1	0.05
NM_002017|NM_001167681	FLI1|EWSR1	2.1	0.04
NM_005739	RASGRP1	2.1	0.005
NM_005608	PTPRCAP	2.1	0.005
NM_018384	GIMAP5	2.0	0.001
NM_006060	IKZF1	2.0	0.01
NM_001164315|NM_025190	ANKRD36|ANKRD36B	2.0	0.04
NM_001803	CD52	2.0	0.02
NM_000439	PCSK1	2.0	0.03
NM_018456	EAF2	2.0	0.01
NM_001040153	SLAIN1	2.0	0.02
NM_005337	NCKAP1L	2.0	0.01

For Peer Review

Ileum DOWN

Identifiler	Gene title	Fold change	p
NM_001807	CEL	-14.1	0.03
NM_022444	SLC13A1	-13.5	0.04
NM_001040442	FABP6	-10.4	0.13
NM_206832	TMIGD1	-7.7	0.07
NM_153021	PLB1	-6.8	0.09
NM_004617	TM4SF4	-6.5	0.21
NM_001081	CUBN	-6.4	0.06
NM_153237	C9orf71	-6.3	0.04
NM_001076|NM_001077	UGT2B15|UGT2B17	-5.8	0.14
NM_001076|NM_001077	UGT2B15|UGT2B17	-5.8	0.15
NM_001077	UGT2B17	-4.8	0.07
NM_033100	CDHR1|PCDH21	-4.2	0.04
NM_000767	CYP2B6	-4.1	0.05
NM_002555|NM_183233	SLC22A18	-4.0	0.01
NM_019893|NM_001079516	ASAH2|ASAH2B|ASAH2C	-3.9	0.02
NM_019893|NM_001079516	ASAH2|ASAH2B|ASAH2C	-3.9	0.30
NM_033553	GUCA2A	-3.9	0.14
NM_001074	UGT2B7	-3.7	0.16
NM_000111	SLC26A3	-3.7	0.11
NM_173077	CPO	-3.7	0.16
NM_017460	CYP3A4	-3.7	0.37
NM_001142462	OSR2	-3.7	0.03
NM_019893|NM_001079516	ASAH2|ASAH2B|ASAH2C	-3.5	0.26
NM_001115131	C6	-3.5	0.02
NM_000777	CYP3A5	-3.5	0.11
NM_005518	HMGCS2	-3.5	0.26
NM_004212	SLC28A2	-3.3	0.38
NM_207373	C10orf99	-3.3	0.22
NM_001045	SLC6A4	-3.2	0.24
NM_000384	APOB	-3.1	0.30
NM_206893	MS4A10	-3.1	0.37
NM_004827	ABCG2	-3.1	0.26
NM_001086	AADAC	-3.1	0.28
NM_001003954	ANXA13	-3.1	0.26
NM_000482	APOA4	-3.0	0.34
NM_001945	HBEGF	-3.0	0.19
NM_178498	SLC5A12	-3.0	0.35

For Peer Review

NM_005073	SLC15A1	-3.0	0.20
NM_000482	APOA4	-3.0	0.34
NM_000340	SLC2A2	-3.0	0.26
NM_000452	SLC10A2	-3.0	0.29
NM_006424	SLC34A2	-3.0	0.10
NM_000040	APOC3	-2.9	0.18
NM_017662	TRPM6	-2.9	0.07
NM_000040	APOC3	-2.9	0.27
NM_001164462	MUC12	-2.9	0.04
NM_021969	NR0B2	-2.9	0.07
NM_000039	APOA1	-2.9	0.13
NM_005925	MEP1B	-2.9	0.32
NM_000770	CYP2C8|CYP2C19	-2.9	0.04
NM_000039	APOA1	-2.9	0.36
NM_080877	SLC34A3	-2.9	0.002
NM_147161|NM_176782	ACOT11|FAM151A	-2.8	0.15
NM_001003841	SLC6A19	-2.8	0.31
NM_001074	UGT2B7	-2.7	0.28
NM_019601	SUSD2	-2.7	0.23
NM_001164462	MUC12	-2.7	0.01
NM_001146108	PTGR1	-2.7	0.15
NM_173354	SIK1	-2.7	0.04
NM_000392	ABCC2	-2.6	0.23
NM_001977	ENPEP	-2.6	0.24
NM_013381	TRHDE	-2.5	0.13
NM_016591	GCNT4	-2.5	0.32
NM_004164	RBP2	-2.5	0.40
NM_000927	ABCB1	-2.5	0.19
NM_004205	USP2	-2.5	0.09
NM_020299	AKR1B10	-2.5	0.26
NM_003167	SULT2A1	-2.5	0.36
NM_007102	GUCA2B	-2.5	0.17
NM_001142564	CNGA1	-2.5	0.001
NM_001944	DSG3	-2.5	0.004
NM_000898	MAOB	-2.4	0.31
NM_032607	CREB3L3	-2.4	0.31
NM_021804	ACE2	-2.4	0.27
NM_152338	ZG16	-2.4	0.28
NM_000775	CYP2J2	-2.4	0.25
NM_001005353	AK3L1	-2.4	0.003

For Peer Review

NM_000846	GSTA2	-2.4	0.26
NM_014905	GLS	-2.4	0.08
NM_002458	MUC5B	-2.4	0.004
NM_020716	GRAMD1B	-2.4	0.20
NM_014270	SLC7A9	-2.4	0.20
NM_002021	FMO1	-2.4	0.23
NM_181785	SLC46A3	-2.3	0.17
NM_004668	MGAM	-2.3	0.20
NM_007180	TREH	-2.3	0.39
NM_032439|NM_001001971	PHYHIPL|FAM13C	-2.3	0.26
NM_001010893	SLC10A5	-2.3	0.22
NM_004696	SLC16A4	-2.3	0.06
NM_006259	PRKG2	-2.3	0.26
NM_000253	MTTP	-2.3	0.34
NM_014053	FLVCR1	-2.3	0.23
NM_152338	ZG16	-2.3	0.28
NM_000151	G6PC	-2.3	0.51
NM_004170	SLC1A1	-2.3	0.19
NM_004133	HNF4G	-2.3	0.21
NM_024743	UGT2A3	-2.2	0.39
NM_173039	AQP11	-2.2	0.24
NM_005624	CCL25	-2.2	0.29
NM_021187	CYP4F11	-2.2	0.32
NM_001631	ALPI	-2.2	0.30
NM_005562	LAMC2	-2.2	0.04
NM_153446	B4GALNT2	-2.2	0.03
NM_025047	ARL14	-2.2	0.04
NM_002614|NR_003377	PDZK1|PDZK1P1	-2.2	0.26
NR_027384	SLC13A2	-2.2	0.38
NM_006017	PROM1	-2.2	0.01
NM_024743	UGT2A3	-2.2	0.34
NM_017675|NM_001171976	CDHR2|PCDH24	-2.2	0.26
NM_000112	SLC26A2	-2.1	0.12
NM_002639	SERPINB5	-2.1	0.04
NM_004235	KLF4	-2.1	0.002
NM_004403	DFNA5	-2.1	0.13
NM_003783	B3GALT2	-2.1	0.02
NM_015888	HOOK1	-2.1	0.07
NM_000463|NM_001072|NM_019075 |NM_021027|NM_007120|NM_019093	UGT1A1|UGT1A6|UGT1A10 |UGT1A9|UGT1A4|UGT1A3	-2.1	0.29

For Peer Review

|NM_019078|NM_019077|NM_019076	|UGT1A5|UGT1A7|UGT1A8		
NM_014227	SLC5A4	-2.1	0.41
NM_015020|NM_001017967	PHLPP2|MARVELD3	-2.1	0.25
NM_152622	MIER3	-2.1	0.07
NM_024989	PGAP1	-2.1	0.06
NM_001082	CYP4F2	-2.1	0.32
NM_014471	SPINK4	-2.1	0.12
NM_153614	DNAJB13	-2.1	0.08
NM_207330	NIPAL1	-2.1	0.06
NM_001112706	SCIN	-2.1	0.19
NM_147164	CNTFR	-2.1	0.12
NM_003399	XPNPEP2	-2.1	0.38
NM_013389	NPC1L1	-2.1	0.56
NM_018713	SLC30A10	-2.1	0.32
NM_182762	MACC1	-2.1	0.16
NM_001104554	PAQR5	-2.1	0.13
NM_014181	HSPC159	-2.1	0.04
NM_022901	LRRC19	-2.1	0.13
NM_001025356	ANO6	-2.1	0.09
NM_000240	MAOA	-2.0	0.31
NM_001098844	TMEM236	-2.0	0.22
NM_001098844	TMEM236	-2.0	0.22
NM_006200	PCSK5	-2.0	0.22
NM_022436	ABCG5	-2.0	0.41
NM_152357	ZNF440	-2.0	0.03
NM_004232	SOCS6	-2.0	0.04
NM_017878	HRASLS2	-2.0	0.28
NM_000949	PRLR	-2.0	0.17
NM_145034	TOR1AIP2	-2.0	0.17
NM_020974	SCUBE2	-2.0	0.23
	CD36	-2.0	0.43

For Peer Review

Supplementary Table S3 legend

Microarray analysis

Total RNA was extracted using standard protocols (Affymetrix). Targets were prepared and hybridized to GeneChip Human Gene 1.0 ST arrays (Affymetrix), according to standard protocols. GeneChip data sets were analyzed using GeneSpring GX 7.3.1 (Agilent). Array data were normalized using robust multi-array analysis considering guanine and cytosine content algorithms.

The gene expression in jejunum was compared between CD (8 samples from 4 patients) and non-IBD patients (8 samples from 4patients). The gene expression in ileum was also compared between CD (4 samples from 2 patients) and non-IBD patients (4 samples from 2patients).

For Peer Review